Competition alters predicted forest carbon cycle responses to nitrogen availability and elevated CO_2: simulations using an explicitly competitive, game-theoretic vegetation demographic model

Ensheng Weng[1,2], Ray Dybzinski[3], Caroline E. Farrior[4], Stephen W. Pacala[5]

[1]Center for Climate Systems Research, Columbia University, New York, NY 10025

[2]NASA Goddard Institute for Space Studies, 2880 Broadway, New York, NY 10025

[3]Institute of Environmental Sustainability, Loyola University Chicago, Chicago, IL 60660

[4] Department of Integrative Biology, University of Texas at Austin, Austin, TX 78712

[5]Department of Ecology & Evolutionary Biology, Princeton University, Princeton, NJ 08544

Corresponding author: Ensheng Weng (wengensheng@gmail.com; phone: 212-678-5585)

Key words: Allocation; Biome Ecological strategy simulator (BiomeE); Competitively-optimal strategy; Game theory; Nitrogen cycle

Abstract: Competition is a major driver of carbon allocation to different plant tissues (e.g. wood, leaves, fine roots), and allocation, in turn, shapes vegetation structure. To improve their modeling of the terrestrial carbon cycle, many Earth system models now incorporate vegetation demographic models (VDMs) that explicitly simulate the processes of individual-based competition for light and soil resources. Here, in order to understand how these competition processes affect predictions of the terrestrial carbon cycle, we simulate forest responses to elevated CO_2 along a nitrogen availability gradient using a VDM that allows us to compare fixed allocation strategies versus competitively-optimal allocation strategies. Our results show that competitive and fixed strategies predict opposite fractional allocation to fine roots and wood, though they predict similar changes in total NPP along the nitrogen gradient. The competitively-optimal allocation strategy predicts decreasing fine root and increasing wood allocation with increasing nitrogen, whereas the fixed allocation strategy predicts the opposite. Although simulated plant biomass at equilibrium increases with nitrogen due to increases in photosynthesis for both allocation strategies, the increase in biomass with nitrogen is much steeper for competitively-optimal allocation due to its increased allocation to wood. The qualitatively opposite fractional allocation to fine roots and wood of the two strategies also impacts the effects of elevated [CO_2] on plant biomass. Whereas the fixed allocation strategy predicts an increase in plant biomass under elevated [CO_2] that is approximately independent of nitrogen availability, competition leads to higher plant biomass response to elevated [CO_2] with increasing nitrogen availability. Our results indicate that the VDMs that explicitly include the effects of competition for light and soil resources on allocation may generate significantly different ecosystem-level predictions of carbon storage than those that use fixed strategies.

1 Introduction

Allocation of assimilated carbon to different plant tissues is a fundamental aspect of plant growth and profoundly affects terrestrial ecosystem biogeochemical cycles (Cannell and Dewar, 1994; Lacointe, 2000). Ecologically, allocation represents an evolutionarily-honed "strategy" of plants that use limited resources and compete with other individuals and consequently drives successional dynamics and vegetation structure (De Kauwe et al., 2014; DeAngelis et al., 2012; Haverd et al., 2016; Tilman, 1988). Biogeochemically, allocation links plant physiological processes, such as photosynthesis and respiration, to biogeochemical cycles and carbon storage of ecosystems (Bloom et al., 2016; De Kauwe et al., 2014). Thus, correctly modeling allocation patterns is critical for correctly predicting terrestrial carbon cycles and Earth system dynamics.

In current Earth System Models (ESMs), the terrestrial carbon cycle is usually simulated by pool-based compartment models that simulate ecosystem biogeochemical cycles as lumped pools and fluxes of plant tissues and soil organic matter (Fig. 1: A) (Emanuel and Killough, 1984; Eriksson, 1971; Parton et al., 1987; Randerson et al., 1997; Sitch et al., 2003). In these models, the dynamics of carbon can be described by a linear system of equations (Koven et al., 2015; Luo et al., 2001; Luo and Weng, 2011; Sierra and Mueller, 2015; Xia et al., 2013):

$$\frac{dX}{dt} = AX + BU \qquad \text{(Eq. 1)}$$

where X is a vector of ecosystem carbon pools, U is carbon input (i.e., Gross Primary Production, GPP), B is the vector of allocation parameters to autotrophic respiration and plant carbon pools (e.g., leaves, stems, and fine roots), and A is a matrix of carbon transfer and turnover. In this system, carbon dynamics are defined by carbon input (U), allocation (B), and residence time and transfer coefficients (A). The allocation schemes (B) are thus embedded in a linear system, or

quasi-linear system if the allocation parameters in B are a function of carbon input (U) or plant carbon pools (X).

The modeling of allocation in this system (i.e., the parameters in vector B) is usually based on plant allometry, biomass partitioning, and resource limitation (De Kauwe et al., 2014; Montané et al., 2017). The allocation parameters are either fixed ratios to leaves, stems, and roots, which may vary among plant functional types (e.g., CENTURY, Parton et al., 1987; TEM, Raich et al., 1991; CASA, Randerson et al., 1997) or are responsive to climate and soil conditions as a way to phenomenologically mimic the shifts in allocation that are empirically observed or hypothesized (e.g., CTEM, Arora and Boer, 2005; ORCHIDEE, Krinner et al., 2005; LPJ, Sitch et al., 2003). These modeling approaches either assume that vegetation is equilibrated (fixed ratios) or average the responses of plant types to changes in environmental conditions as a collective behavior. Thus, the carbon dynamics in these models can be constrained by selecting appropriate parameters of allocation, turnover rates, and transfer coefficients to fit the observations (Friend et al., 2007; Hoffman et al., 2017; Keenan et al., 2013).

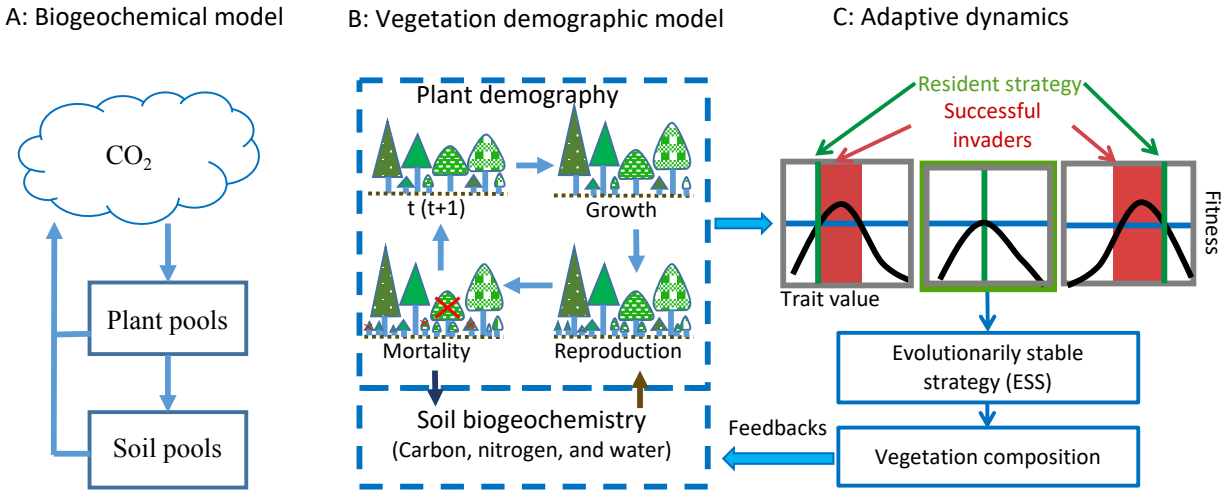

Figure 1 Hierarchical structure of vegetation models

79 To predict transient changes in vegetation structure and composition in response to climate
80 change, vegetation demographic models (VDMs) that are able to simulate transient population
81 dynamics are incorporated into ESMs (Fisher et al., 2018; Scheiter and Higgins, 2009).
82 Generally, VDMs explicitly simulate demographic processes, such as plant reproduction, growth,
83 and mortality, to generate the dynamics of populations (Fig. 1: B). To speed computations and
84 minimize complexity, groups of individuals are usually modeled as cohorts. With multiple
85 cohorts and PFTs, VDMs can bring plant functional diversity and adaptive dynamics into ESMs
86 when explicitly simulating individual-based competition for different resources and vegetation
87 succession and thus predict dominant plant traits changes with environmental conditions and
88 ecosystem development (Scheiter et al., 2013; Scheiter and Higgins, 2009; Weng et al., 2015).

89 The combinations of plant traits represent the competition strategies at different stages of
90 ecosystem development. Evolutionarily, a strategy that can outcompete all other strategies in the
91 environment created by itself will be dominant. This strategy is called an evolutionarily stable
92 strategy or a competitively-optimal strategy (McGill and Brown, 2007). In VDMs,
93 competitively-optimal strategies can therefore be reasonably predicted based on the costs and
94 benefits of different strategies (i.e., combinations of plant traits) through their effects on
95 demographic processes (i.e., fitness) and ecosystem biogeochemical cycles (Fig. 1:C) (e.g.,
96 Farrior et al., 2015; Weng et al., 2015).

97 The dynamics of plant traits can substantially change predictions of ecosystem
98 biogeochemical dynamics since they change the key parameters of vegetation physiological
99 processes and soil organic matter decomposition (e.g., Dybzinski et al., 2015; Farrior et al.,
100 2015; Weng et al., 2017). Therefore, the key parameters that are used to estimate carbon
101 dynamics in the linear system model (Eq. 1), such as allocation (B) and residence times in

different carbon pools (matrix A, which includes coefficients of carbon transfer and turnover time) become functions of competition strategies that vary with environment and carbon input. In addition, the turnover of vegetation carbon pools becomes a function of allocation, leaf longevity, fine root turnover, and tree mortality rates, which change with vegetation succession and the most competitive plant traits. These changes make the system nonlinear and can lead to large biases within the framework of the compartmental pool-based models as represented by Eq. (1) (Sierra et al., 2017; Sierra and Mueller, 2015). Because of the high complexity associated with demographic and competition processes, the model predictions are usually sensitive to the parameters in these processes and are of high uncertainty (e.g., Pappas et al., 2016).

In contrast to their implementation in the more complicated VDMs discussed above, models of competitively-dominant plant strategies using much simpler model structures and assumptions can sometimes be solved analytically (Dybzinski et al., 2011, 2015; Farrior et al., 2013, 2015). Although simplified, such models can pin-point the key processes that improve the predictive power of simulation models (Dybzinski et al., 2011; Farrior et al., 2013, 2015), allowing them to help researchers formulate model processes and understand the simulated ecosystem dynamics in ESMs. For example, the analytical model derived by Farrior et al. (2013) that links interactions between ecosystem carbon storage, allocation, and water stress at elevated CO_2 sheds light on the otherwise inscrutable processes leading to varied soil water dynamics in a land model coupled with an VDM (Weng et al., 2015). Recognizing the benefit, Weng et al. (2017) included both a simplified analytical model and a more complicated VDM to understand competitively optimal leaf mass per area, competition between evergreen and deciduous plant functional types, and the resulting successional patterns.

In this study, we use a stand-alone simulator derived from the LM3-PPA model (Weng et al., 2017, 2015) to show how forests respond to elevated CO_2 and nitrogen availability via different competitively-optimal allocation strategies. The model is an individual-based vegetation demographic model, whose vegetation demographic scheme has been coupled into the land model of the Geophysical Fluid Dynamical Laboratory's Earth System Model (Shevliakova et al., 2009; Weng et al., 2015) and NASA Goddard Institute for Space Study's Earth system model, ModelE (Schmidt et al., 2014). Using this model, we simulate the shifts in competitively optimal allocation strategies in response to elevated CO_2 at different nitrogen levels based on insights from the analytical model derived by Dybzinski et al. (2015). Dybzinski et al.'s (2015) model predicts that increases in carbon storage at elevated CO_2 relative to storage at ambient CO_2 are largely independent of total nitrogen because of an increasing shift in carbon allocation from long-lived, low-nitrogen wood to short-lived, high-nitrogen fine roots under elevated CO_2 with increasing nitrogen availability. Here, we analyze the simulated ecosystem carbon cycle variables (gross and net primary production, allocation, and biomass) of separate mono- and polyculture model runs. In the monoculture runs, ecosystem properties are the result of the prescribed allocation strategies of a given PFT, analogous to the fixed allocation schemes of most VDMs (see above). In the polyculture runs, competition between the different allocation strategies results in succession and the eventual dominance of the most competitive allocation strategy for a given nitrogen availability and CO_2 level. Since everything else in the model is identical, we are able to compare the predictions of single **fixed strategies** with **competitively-optimal allocation strategies** by comparing the ecosystem properties of these two types of runs.

2 Methods and Materials

2.1 BiomeE model overview

We used a stand-alone ecosystem simulator (Biome Ecological strategy simulator, BiomeE) to conduct simulation experiments. BiomeE is derived from the version of LM3-PPA used in Weng *et al*. (2017). In this version, we simplified the processes of energy transfer and soil water dynamics of LM3-PPA (Weng et al., 2015) but still retained the key features of plant physiology and individual-based competition for light, soil water, and, via the decomposition of soil organic matter, nitrogen (Fig. 2). In this model, individual trees are represented as sets of *cohorts* of similar size trees and are arranged in different vertical canopy layers according to their height and crown area following the rules of the Perfect Plasticity Approximation (PPA) model (Strigul et al., 2008). Sunlight is partitioned into these canopy layers according to Beer's law. Thus, a key parameter for light competition, critical height, is defined; all the trees above this context-dependent height get full sunlight and all trees below this height are shaded by the upper layer trees.

Each tree consists of seven pools: leaves, fine roots, sapwood, heartwood, fecundity (seeds), and non-structural carbohydrates and nitrogen (NSC and NSN, respectively) (Fig. 2: b). The carbon and nitrogen in plant pools enter the soil pools with the mortality of individual trees and the turnover of leaves and fine roots. There are three soil organic matter (SOM) pools for carbon and nitrogen: fast-turnover, slow-turnover, and microbial pools, along with a mineral nitrogen pool for mineralized nitrogen in soil. The simulation of SOM decomposition and nitrogen mineralization is based on the models of Gerber *et al*. (2010) and Manzoni *et al*. (2010) and described in detail in Weng et al. (2017). The decomposition rate of a SOM pool is determined by the basal turnover rate together with soil temperature and moisture. The nitrogen

mineralization rate is a function of decomposition rate and the C:N ratio of the SOM. Microbes must consume more carbon in the high C:N ratio SOM pool to get enough nitrogen and must release excessive nitrogen in the low C:N ratio SOM pool to get enough carbon for energy (Weng *et al*. 2017).

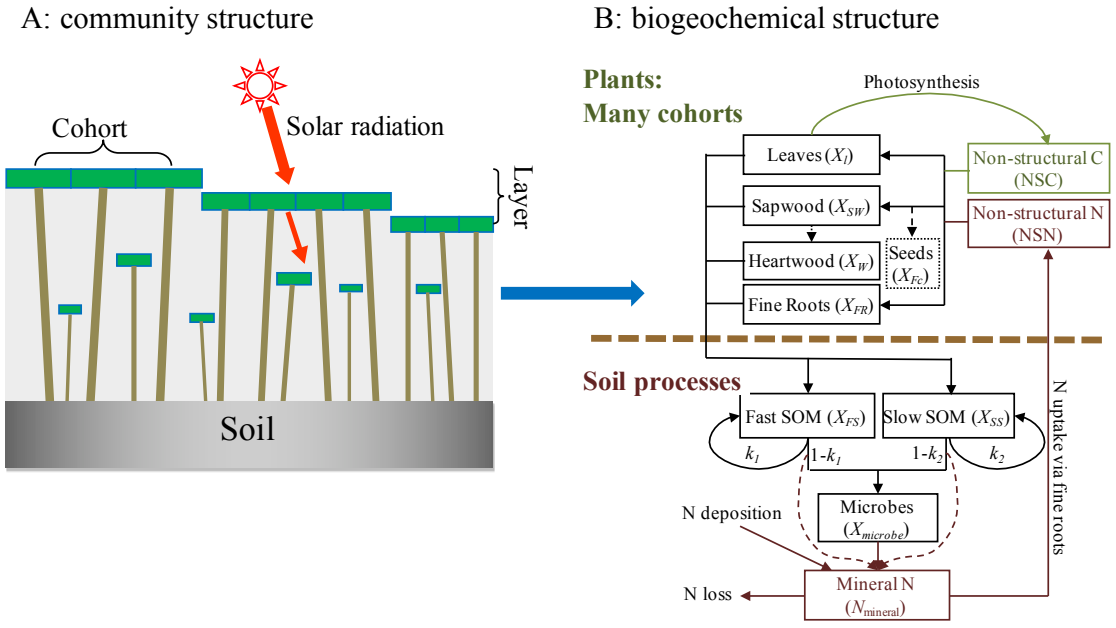

Figure 2. Model structure of BiomeE

Panel A: vegetation structure: trees organize their crowns into canopy layers according to both their height and their crown area following the rules of the PPA model, which mechanistically models light competition. Panel B: Biogeochemical structure and compartmental pools. The green, brown, and black lines are the flows of carbon, nitrogen, and coupled carbon and nitrogen, respectively. The green box is for carbon only. The brown boxes are N pools. The black boxes are for both carbon and nitrogen pools, where *X* can be C (carbon) and N (nitrogen). The C:N ratios of leaves, fine roots, seeds, and microbes are fixed. The C:N ratios of woody tissues, fast soil organic matter (SOM), and slow SOM are flexible. Only one tree's C and N pools are shown in this figure. The model can have multiple cohorts of trees, which share the same pool structure. The dashed line separates the plant and soil processes.

186 **Table 1 Model parameters**

Symbol	Definition	Unit	Default value
α_Z	Parameter of tree height	m $m^{-0.5}$	36
θ_Z	Diameter exponent of tree height	-	0.5
Λ	Taper factor	-	0.75
ρ_W	Wood density	kgC m^{-3}	300
α_C	Parameter of crown area	m $m^{-1.5}$	150
θ_C	Diameter exponent of crown area	-	1.5
l^*	Target crown leaf area layers (crown leaf area index)	m^2 m^{-2}	3.5
σ	Leaf mass per unit area	kgC m^{-2}	0.14
γ	Specific root area, calculated from root radius and density	m^2 kgC^{-1}	34.5
φ_{RL}	Ratio of target fine root area to target leaf area	m^2 m^{-2}	Vary with PFTs
α_{CSA}	ratio of target sapwood cross-sectional area to target leaf area	m^2 m^{-2}	0.2E-4
$f_{U,max}$	Maximum mineral N absorption rate	$hour^{-1}$	0.5
K_{FR}	Root biomass at which the N-uptake rate is half of the maximum	kgC m^{-2}	0.3
$CN_{L,0}$	Target C:N ratio of leaves	kgC kgN^{-1}	76.5(Function of LMA)
$CN_{FR,0}$	Target C:N ratio of fine roots	kgC kgN^{-1}	60
$CN_{W,0}$	Target C:N ratio of wood	kgC kgN^{-1}	350
$CN_{F,0}$	Target C:N ratio of seeds	kgC kgN^{-1}	20
f_1	Supply rate of NSC and NSN	-	1/(3*365)
f_2	Maximum fraction of NSC and NSN used for growth in a day	-	0.02
$f_{LFR,max}$	Maximum fraction of available carbon allocated to leaves and fine roots	-	0.85
v	Fraction of carbon converted to seeds	-	0.1
$r_{D/S}$	Nitrogen-limiting factor	-	Solve by the model (Eqs 9 and 10)

187

188 Plant growth and reproduction are driven by the carbon assimilation of leaves via
189 photosynthesis, which is in turn dependent on water and nitrogen uptake by fine roots. The
190 photosynthesis model is identical to that of LM3-PPA (Weng et al., 2015), which is a simplified
191 version of Leuning model (Leuning et al., 1995). This model first calculates photosynthesis rate,

stomatal conductance, and water demand of the leaves of each tree (cohort) in the absence of soil water limitation. Then, it calculates available water supply and reduces the demand-based assimilation and stomatal conductance accordingly if water supply is less than water demand. Assimilated carbon enters into the NSC pool and is subsequently used for respiration, growth, and reproduction. (Please see Supplementary Information I for details of this model).

Empirical allometric equations relate woody biomass (including coarse roots, bole, and branches), crown area, and stem diameter. The individual-level dimensions of a tree, *i.e.*, height (Z), biomass (S), and crown area (A_{CR}) are given by empirical allometries (Dybzinski et al., 2011; Farrior et al., 2013):

$$Z(D) = \alpha_Z D^{\theta_Z}$$
$$S(D) = 0.25\pi\Lambda\rho_W\alpha_Z D^{2+\theta_Z} \quad \text{(Eq. 2)}$$
$$A_{CR}(D) = \alpha_c D^{\theta_c}$$

where Z is tree height, D is tree diameter, S is total woody biomass carbon (including bole, coarse roots, and branches) of a tree, α_c and α_Z are PFT-specific constants, θ_c=1.5 and θ_Z=0.5 (Farrior et al., 2013) (although they could be made PFT-specific if necessary), π is the circular constant, Λ is a PFT-specific taper constant, and ρ_W is PFT-specific wood density (kg C m^{-3}) (Table 1).

We set *targets* for leaf (L^*), fine root (FR^*), and sapwood cross-sectional area (A_{SW}^*) that govern plant allocation of non-structural carbon and nitrogen during growth. These *targets* are related by the following equations based on the assumption of the pipe model (Shinozaki, Kichiro et al., 1964):

$$L^*(D,p) = l^* \cdot A_{CR}(D) \cdot \sigma \cdot p(t)$$
$$FR^*(D) = \varphi_{RL} \cdot l^* \cdot \frac{A_{CR}(D)}{\gamma} \quad \text{(Eq. 3)}$$
$$A^*_{SW}(D) = \alpha_{CSA} \cdot l^* \cdot A_{CR}(D)$$

where L^* (D, p), $FR^*(D)$, and $A^*_{SW}(D)$ are the targets of leaf mass (kg C/tree), fine root biomass (kg C/tree), and sapwood cross sectional area (m^2/tree), respectively, at tree diameter D; l^* is the target leaf area per unit crown area of a given PFT; A_{CR}(D) is the crown area of a tree with diameter D; σ is PFT-specific leaf mass per unit area (LMA); and $p(t)$ is a PFT-specific function ranging from zero to one that governs leaf phenology (Weng et al., 2015); φ_{RL} is the target ratio of total root surface area to the total leaf area; γ is specific root area; and α_{CSA} is an empirical constant (the ratio of sapwood cross-sectional area to target leaf area). The phenology function p(t) takes values 0 (non-growing season) or 1 (growing season) following the phenology model of LM3-PPA (Weng et al., 2015). The onset of a growing season is controlled by two variables, growing degree days (GDD), and a weighted mean daily temperature (T_{pheno}), while the end of a growing season is controlled by T_{pheno}. (Please see Supplementary Information I for details of the phenology model)

Nitrogen uptake

The rate of nitrogen uptake (U, g N m^{-2} $hour^{-1}$) from the soil mineral nitrogen pool is an asymptotically increasing function of fine root biomass density ($C_{\text{FR,total}}$, kg C m^{-2}), following McMurtrie *et al*. (2012)

$$U = f_{\text{U,max}} \cdot N_{\text{mineral}} \cdot \frac{C_{\text{FR,total}}}{C_{\text{FR,total}} + K_{FR}}, \quad \text{(Eq. 4)}$$

where, N_{mineral} is the mineral N in soil (g N m^{-2}), $f_{\text{U,max}}$ is the maximum rate of nitrogen absorption per hour when $C_{\text{FR,total}}$ approaches infinity, K_{FR} is a shape parameter (kg C m^{-2}) at

which the nitrogen uptake rate is half of the parameter $f_{U,max}$. The nitrogen uptake rate of an individual tree (U_{tree}, kg N hour^{-1} tree^{-1}) is calculated as follows:

$$U_{\text{tree}} = U \cdot \frac{C_{\text{FR,tree}}}{C_{\text{FR,total}}}, \quad \text{(Eq. 5)}$$

where, $C_{FR,tree}$ is the fine root biomass of a tree (kgC tree^{-1}). The nitrogen absorbed by roots enters into the NSN pool and then is allocated to plant tissues through plant growth.

Allocation and plant growth

The partitioning of carbon and nitrogen into the plant pools (*i.e.*, leaves, fine roots, and sapwood) is limited by the allometric equations, targets of leaves, fine roots, and sapwood cross-sectional area, and the stoichiometry (i.e., C:N ratios) of these plant tissues. At a daily time step, the model calculates the amount of carbon and nitrogen that are available for growth according to the total NSC and NSN and current leaf and fine root biomass. Basically, the available NSC (G_C) is the summation of a small fraction (f_1) of the total NSC in an individual plant and the differences between the targets of leaf and fine roots and their current biomass capped by a larger fraction (f_2) of NSC (Eq. 6.1). The available NSN (G_N) is analogous to that of the NSC and meets approximately the stoichiometrical requirement of plant tissues (Eq. 6.2).

$$G_C = \min\left(f_1 NSC + L^* + FR^* - L - FR, f_2 NSC\right) \quad \text{(Eq. 6.1)}$$

$$G_N = \min\left(f_1 NSN + N_L^* + N_{FR}^* - N_L - N_{FR}, f_2 NSN,\right) \quad \text{(Eq. 6.2)}$$

where L^* and FR^* are the targets of leaves and fine roots, respectively (see Eq. 3); L and FR are current leaf and fine roots biomass, respectively; N_L^* and N_{FR}^* are nitrogen of leaves and fine roots at their targets according to their target C:N ratios. The parameter f_2 gives the daily availability of NSC during periods of leaf flush at the beginning of a growing season and f_1

normal growth of stems after plant leaves and fine roots approach their targets. Usually, parameter f_1 is much greater than f_2. We let f_1=0.02 and f_2= 1/(365x3) in this study.

The allocation of the available NSC (i.e., G_C) to wood (G_W), leaves (G_L), fine roots (G_{FR}), and seeds (G_F) follows the equations below (Eq. 7). These equations describe the mass growth of plant tissues with nitrogen effects on the carbon allocation between high-nitrogen tissues and low-nitrogen tissues (wood) for maximizing leaves and fine roots growth (G_L and G_{FR}, respectively), optimizing carbon usage at given nitrogen supply (G_N), and keeping the tissues at their target C:N ratios.

$$G_C \geq G_W + G_L + G_{FR} + G_F \quad \text{(Eq. 7.1)}$$

$$G_N \geq \frac{G_L}{CN_{L,0}} + \frac{G_{FR}}{CN_{FR,0}} + \frac{G_F}{CN_{F,0}} + \frac{G_W}{CN_{W,0}} \quad \text{(Eq. 7.2)}$$

$$\frac{(FR+G_{FR})\gamma}{(L+G_L)/\sigma} = \varphi_{RL} \quad \text{(Eq. 7.3)}$$

$$G_L + G_{FR} = Min\begin{pmatrix} L^* + FR^* - L - FR, \\ f_{LFR,max}\, G_C \end{pmatrix} \cdot r_{S/D} \quad \text{(Eq. 7.4)}$$

$$G_F = \left[G_C - Min\begin{pmatrix} L^* + FR^* - L - FR, \\ f_{LFR,max}\, G_C \end{pmatrix} r_{S/D}\right] \cdot v \cdot r_{S/D} \quad \text{(Eq. 7.5)}$$

$$G_W = \left[G_C - Min\begin{pmatrix} L^* + FR^* - L - FR, \\ f_{LFR,max}\, G_C \end{pmatrix} r_{S/D}\right] \cdot (1 - v \cdot r_{S/D}) \quad \text{(Eq. 7.6)}$$

where, $CN_{L,0}$, $CN_{FR,0}$, $CN_{F,0}$, and $CN_{W,0}$ are the target C:N ratios of leaves, fine roots, seeds, and sapwood, respectively; γ is specific root area (m^2 kgC^{-1}); σ is leaf mass per unit area (kg C m^{-2}); $f_{LFR,max}$ is the maximum fraction of G_C for leaves and fine roots (0.85 in this study); v is the fraction of left carbon for seeds (0.1 in this study); $r_{S/D}$ is a nitrogen-limiting factor ranging from 0 (no nitrogen for leaves, fine roots, and seeds) to 1 (nitrogen available for full growth of leaves, fine roots, and seeds). The parameter $r_{S/D}$ controls the allocation of G_C and G_N to the four plant pools (Eq. 7.1). It can be analytically solved (Eqs. 8 and 9).

$$r_{S/D} = Min\left[1, Max\left(0, \frac{G_N - G_C/CN_W}{N_{demand} - G_C/CN_W}\right)\right], \quad \text{(Eq. 8)}$$

where, N_{demand} is the potential nitrogen demand for plant growth at $r_{S/D}$=1 (i.e., no nitrogen limitation).

$$N_{demand} = \frac{\gamma\sigma\left[FR + Min\left(\begin{matrix}L^* + FR^* - L - FR, \\ f_{LFR,max}\, G_C\end{matrix}\right)\right] - \varphi_{RL} L}{(\gamma\sigma + \varphi_{RL}) CN_L} + \frac{\varphi_{RL}\left[L + Min\left(\begin{matrix}L^* + FR^* - L - FR, \\ f_{LFR,max}\, G_C\end{matrix}\right)\right] - \gamma\sigma L}{(\gamma\sigma + \varphi_{RL}) CN_{FR}} + \frac{v\left[G_C - Min\left(\begin{matrix}L^* + FR^* - L - FR, \\ f_{LFR,max}\, G_C\end{matrix}\right)\right]}{CN_F} + \frac{(1-v)\left[G_C - Min\left(\begin{matrix}L^* + FR^* - L - FR, \\ f_{LFR,max}\, G_C\end{matrix}\right)\right]}{CN_W}. \quad \text{(Eq. 9)}$$

When $G_N \geq N_{demand}$ ($r_{S/D}$ = 1), there is no nitrogen limitation, and all the G_C will be used for plant growth and the allocation follows the rules of the carbon only model (Eqs 7.4~7.6 as $r_{S/D}$ = 1). The excessive nitrogen ($G_N - N_{demand}$) will be returned to the NSN pool. When $G_C/CN_{W,0} < G_N < N_{demand}$ (i.e., $0 < r_{S/D} < 1$), all G_C and G_N will be used in new tissue growth; however, the leaves and fine roots cannot reach their targets at this step. When $G_N \leq G_C/CN_{W,0}$ ($r_{S/D}$ = 0), all the G_N will be allocated to sapwood and the excessive carbon ($G_C - G_N CN_{W,0}$) will be returned to NSC pool. This is a very rare case since a low G_N leads to low leaf growth, reducing G_C before the case $G_N < G_C/CN_{W,0}$ happens. Therefore, in most cases, Eq. 7.1 is: $G_C = G_W + G_L + G_{FR} + G_F$.

Allocation to wood tissues (G_W) drives the growth of tree diameter, height, and crown area and thus increases the targets of leaves and fine roots (Eq. 3). By differentiating the stem biomass allometry in Eq. 2 with respect to time, using the fact that dS/dt equals the carbon allocated for wood growth (G_W), we have the diameter growth:

$$\frac{dD}{dt} = \frac{G_W}{0.25\pi\Lambda\rho_W\alpha_z(2+\theta_z)D^{1+\theta_Z}} \quad \text{(Eq. 10)}$$

This equation transforms the mass growth to structural changes in tree architecture. With an updated tree diameter, we can calculate the new tree height and crown area using allometry equations (Eq. 2) and targets of leaf and fine root biomass (Eq. 3) for the next growth step.

Overall, this is a flexible allocation scheme and still follows the major assumptions in the previous version of LM3-PPA (Weng, et al., 2015, 2017). This allocation scheme prioritizes the allocation to leaves and fine roots, maintains a minimum growth rate of stems, and keeps the constant area ratio of fine roots to leaves. Based on these allocation rules, the average allocation of carbon and nitrogen to leaves, fine roots, and wood over a growing season are governed by the targets for the leaf area per unit crown area (i.e., crown leaf area index, l^*) and fine root area per unit leaf area (φ_{RL}). Since the crown leaf area index, l^*, is fixed in this study, φ_{RL} is the key parameter determining the relative allocation of carbon to fine roots and stems. A high φ_{RL} means a high relative allocation to fine roots and therefore low relative allocation to stems, and *vice versa*. Note, here φ_{RL} is fixed for each PFT and will remain so for all the model runs.

The process of choosing a context-dependent competitively dominant φ_{RL} will take place after finding the fitness of each φ_{RL} in monoculture and in competition with other PFTs (*i.e.*, different values of φ_{RL}). The competitively optimal strategy is the one that can successfully exclude all others in the processes of competition and succession, but it is not necessarily the one that maximizes production in monoculture. For example, each φ_{RL} creates an environment of light profile and soil nitrogen in its monoculture. Other φ_{RL} PFTs may have higher fitness in this environment than the one that creates it. Only the competitively dominant strategy has the highest fitness in the environment it creates (Fig. 1: C).

2.2 Site and Data

297 Data pertaining to vegetation, climate, and soil at Harvard Forest (Aber et al., 1993; Hibbs, 1983;
298 Urbanski et al., 2007) were used to design the plant functional types (PFTs) and ecosystem
299 nitrogen levels used in the simulation experiments, to drive the model, and to calibrate model
300 parameters. Harvard Forest is located in Massachusetts, USA (42.54°, -72.17°). The climate of
301 Harvard Forest is cool temperate with annual precipitation 1050 mm, distributed fairly evenly
302 throughout the year. The annual mean temperature is 8.5 °C with a high monthly mean
303 temperature of 20°C in July and a low of -7°C in January. The soils are mainly sandy loam with
304 average depth around 1 m and are moderately well drained in most areas. In forest sites, soil
305 carbon is around 8 kg C m^{-2} and nitrogen 300 g N m^{-2} (Compton and Boone, 2000). The
306 vegetation is deciduous broadleaf/mixed forest with major species red oak (*Quercus rubra*), red
307 maple (*Acer rubrum*), black birch (*Betula lenta*), white pine (*Pinus strobus*), and hemlock (*Tsuga*
308 *canadensis*) (Compton and Boone, 2000; Savage et al., 2013). The data used to drive our model
309 runs are gap-filled hourly meteorological data at Harvard Forest from 1991 to 2006, obtained
310 from North American Carbon Program (NACP) Site-Level Synthesis datasets (Barr et al., 2013).
311
312 **2.3 Simulation experiments**
313 We set two atmospheric CO_2 concentration ($[CO_2]$) levels: 380 ppm and 580 ppm, and
314 eight ecosystem total nitrogen levels (ranging from 114.5 g N m^{-2} to 552 g N m^{-2} at the interval
315 of 62.5 g N m^{-2}) by assigning the initial content of the slow SOM pool for our simulation
316 experiments (Table 2). This range covers the soil nitrogen content at Harvard Forest (Compton
317 and Boone, 2000; Melillo et al., 2011). The nitrogen cycles through the plant and soil pools and
318 is redistributed among them via plant demographic processes, soil carbon transfers, and plant
319 uptake. In all the simulation experiments, we assume the ecosystem has no nitrogen inputs and

no outputs for convenience since we already have eight total nitrogen levels to represent the consequences of different nitrogen input and output processes at an equilibrium state. The PFTs were based on an evergreen needle-leaved tree PFT with different leaf to fine root area ratios, φ_{RL}, in the range from 1 to 8 (Table 2). Simply stated, the PFTs we investigate only differ in parameter φ_{RL}.

We define the model runs initialized with only one fixed-φ_{RL} PFT as "monoculture runs" although the actual allocation of carbon to different plant tissues varies with [CO_2] concentration and ecosystem nitrogen availability. We define the model runs initialized with multiple PFTs as "polyculture runs" (eight PFTs with different φ_{RL} at the beginning, although many are driven to extinction during a given model run). We conducted one set of monoculture runs and two sets of polyculture runs (Table 2).

Table 2 Simulation experiments

Type	Model runs	Initial PFT(s) φ_{RL}	Ecosystem total nitrogen levels	CO_2 concentration [CO_2]
Monoculture runs	One model run per combination of PFT (φ_{RL}), nitrogen level, and CO_2 concentration	One of the following PFTs: φ_{RL}= 1, 2, 3, 4, 5, 6, 7, or 8	Eight levels ranging from 114.5 g N m^{-2} to 552 g N m^{-2} at the interval of 62.5 g N m^{-2}: 114.5 g N m^{-2}, 177 g N m^{-2}, 239.5 g N m^{-2}, 302 g N m^{-2}, 364.5 g N m^{-2}, 427 g N m^{-2}, 489.5 g N m^{-2},	Ambient: 380 ppm Elevated: 580 ppm
Polyculture runs I	One model run per combination of nitrogen level and CO_2 concentration	All the PFTs (φ_{RL}= 1~ 8) used in the monoculture runs		
Polyculture runs II	One model run per combination of nitrogen level and CO_2 concentration	Eight PFTs with φ_{RL} ranging from 4.5-0.5*i* to 8.5-0.5*i* at the interval of 0.5, where *i* denotes the eight nitrogen		

	levels from 114.5 to 552 gN m^{-2}.	552 g N m^{-2}	

In the monoculture runs, we run the full combinations of eight PFTs with root/leaf area ratios (φ_{RL}) from 1 to 8, eight ecosystem total nitrogen levels, and two CO_2 concentrations [CO_2] (380 ppm and 580 ppm) (Table 2). For the eight PFTs, only those with φ_{RL} <=6 survived at ambient [CO_2] (380 ppm) because the carbon consumed by fine roots exceeded what leaves provided at φ_{RL}>6. The monoculture runs are for exploring the model predictions of gross primary production (GPP), net primary production (NPP), allocation, and biomass at equilibrium with fixed φ_{RL} and ecosystem total nitrogen levels, analogous to the functional relationship schemes used in many ecosystem models (e.g., De Kauwe et al., 2014).

In polyculture runs I, we used the same PFTs as in the monoculture runs, where their φ_{RL} varies from 1 to 8 at the interval of 1.0 and the ecosystem total nitrogen levels are the same as those used in the monoculture runs (Table 2). This set of polyculture runs was used to explore successional patterns at both ambient and elevated [CO_2] concentrations (380 ppm and 580 ppm, respectively). However, this set of model runs could not show the details of equilibrium plant biomass and allocation patterns along the nitrogen gradient because of the large intervals between the φ_{RL} values.

To achieve greater resolution in our competition predictions, we designed the polyculture runs II using a dynamic PFT combination scheme according to the ranges of φ_{RL} obtained from the polyculture runs I that could survive at a particular nitrogen level at both CO_2 concentrations. For each nitrogen level, we set eight PFTs with φ_{RL} that varied in a range 3.5 (e.g., $x \sim x$+3.5) at the interval of 0.5, starting with the highest φ_{RL} of 8.0 at the lowest N level (114.5 g N m^{-2}) and decreasing 0.5 per level of increase in ecosystem total N. Let i=1, 2, …, 8 denote the eight N

355 levels from 114.5 to 552 g N m^{-2}, the φ_{RL} of the eight PFTs at each level are (5.0-0.5*i*, 5.5-
356 0.5*i*, …, 8.5-0.5*i*) (Table 2). For example, at the nitrogen of 114.5 g N m^{-2} (i = 1), the φ_{RL} of the
357 eight PFTs are 4.5, 5.0, …, 8.0 and at 177 g N m^{-2} (i = 2), they are 4.0, 4.5, …, 7.5.
358 For both monoculture and polyculture runs, visual inspection indicated that stands had
359 reached equilibrium after ~1200 years. To be conservative, we present equilibrium data by
360 averaging model properties between years 1400 and 1800. We compared simulated equilibrium
361 gross primary production (GPP), net primary production (NPP), allocation (both absolute amount
362 of carbon and fractions of the total NPP), and plant biomass of the polyculture runs II with those
363 from the monoculture runs. We used the results from one PFT (φ_{RL}=4) to highlight the
364 differences of plant responses with competitively optimal allocation strategies obtained from the
365 polyculture runs II.
366
367 **3 Results**
368 In the monoculture runs, GPP and NPP increase by a factor of three along the gradient of
369 nitrogen used in this study (114.5 - 552 g N m^{-2}) at both ambient (Fig. 3) and elevated [CO_2]
370 (Figs. S1). The magnitude of differences in GPP and NPP due to differences in fixed allocation
371 within a given nitrogen level is comparable to the magnitude of differences in GPP and NPP due
372 to nitrogen level within a given fixed allocation strategy (Fig. 3: a and b) when φ_{RL} is in the
373 range that allows plants to grow normally (1~5 in the case of ambient [CO_2]). As prescribed by
374 the definition of φ_{RL}, allocation of NPP to fine roots increases with φ_{RL} in monoculture runs (Fig.
375 3: c). As a consequence, allocation of NPP to wood decreases as φ_{RL} increases (Fig. c: d).
376 Allocation to leaves does not change much with φ_{RL}. (Fig. 3: e, note differences in scale).
377 Correspondingly, plant biomass at equilibrium decreases with φ_{RL} (Fig. 3: f). The effects of

nitrogen on the allocation of carbon to fine roots and wood follow our allocation model assumptions because *proportionally* more carbon is allocated to low-nitrogen woody tissues in our model when nitrogen is limited. However, the amplitude of changes in GPP and NPP induced by nitrogen availability is lower than the amplitude of changes resulting from different values of φ_{RL} in the monoculture runs.

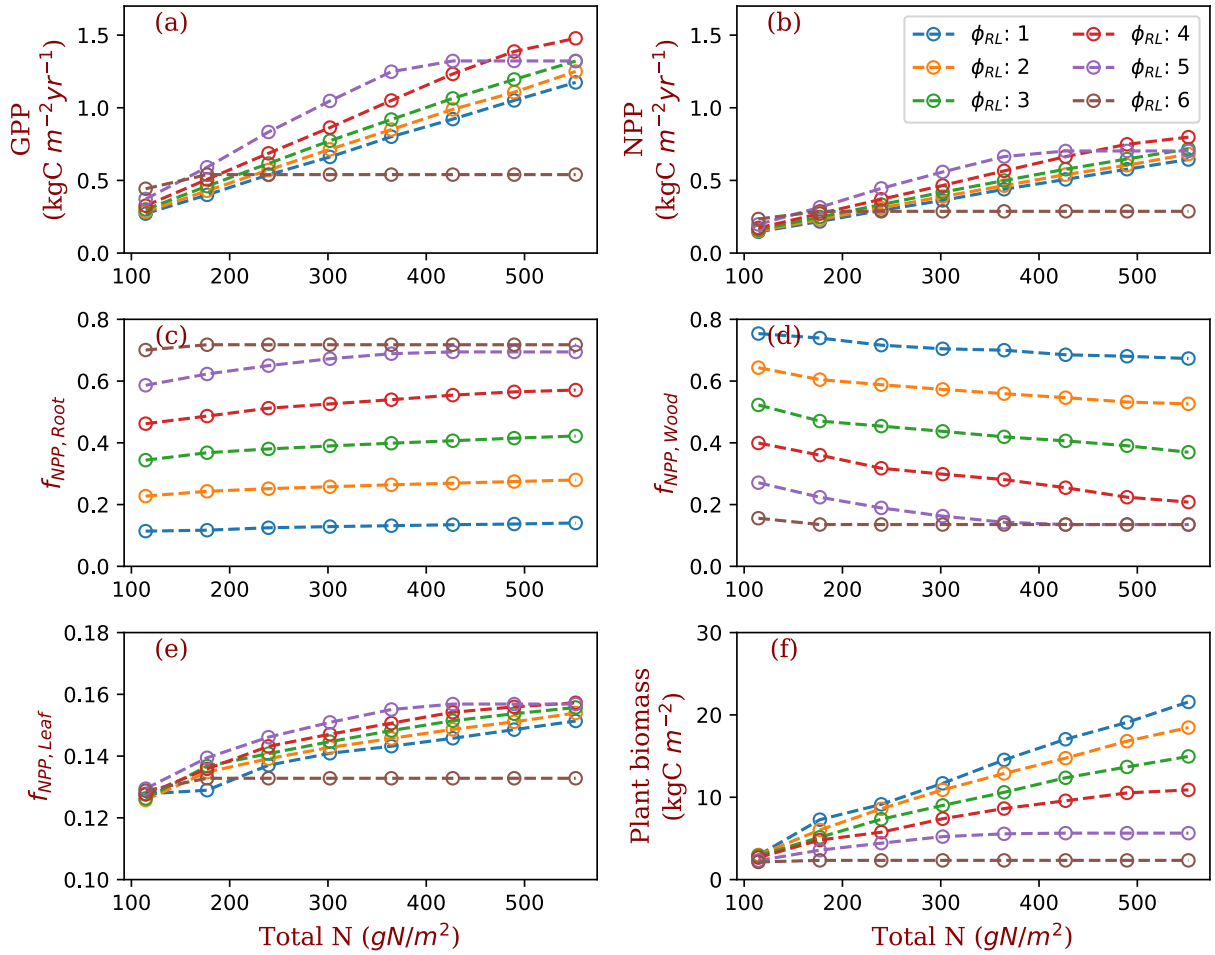

Figure 3. GPP, NPP, Allocation and Plant biomass at equilibrium state simulated by monoculture runs. GPP: Gross primary production; NPP: Net primary production; $f_{NPP,x}$: the fraction of NPP allocated to x, where x is Root (fine roots), Leaf (leaves in crown), or Wood (including tree trunk, stems, and coarse roots). The data are from the averages of the model run

388 years from 1400 and 1800. Each model run is initiated with one PFT with fixed ratio of fine root
389 area to leaf area (φ_{RL}).

390

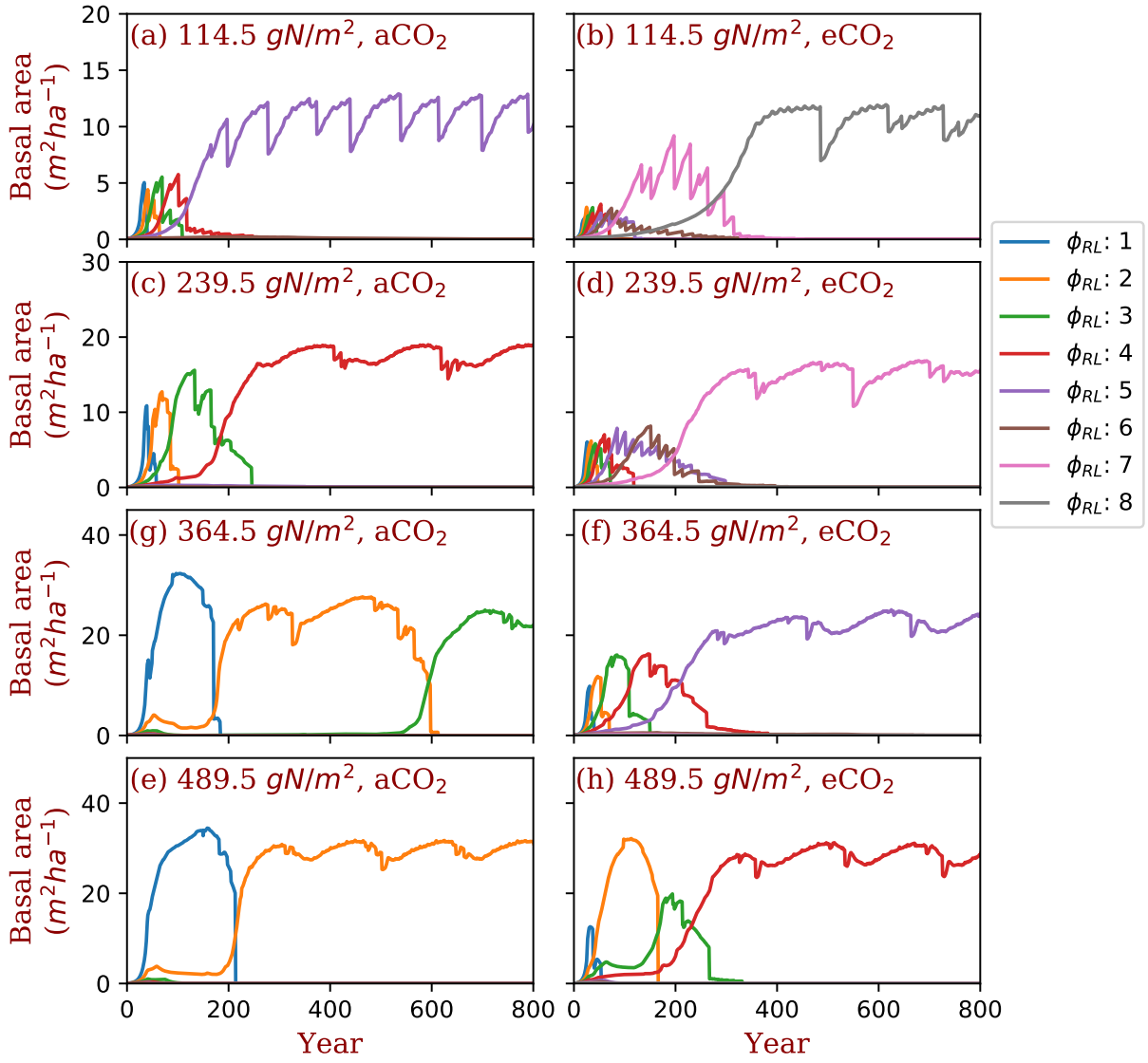

391

392 **Figure 4 Successional patterns of polyculture runs I at ambient and elevated CO2**
393 **concentrations**.

394

395 We used two sets of polyculture runs to look for the φ_{RL} that is closest to the competitively
396 optimal (i.e., evolutionarily stable strategy). In the polyculture runs I, where φ_{RL} ranges from 1 to

8 at all nitrogen levels, the winning strategy (φ_{RL}) increases from 5 to 2 as the total nitrogen increases from 114.5 g N m^{-2} to 489.5 g N m^{-2} at ambient CO_2 (380 ppm) (Fig. 4: a, c, g, e). Elevated CO_2 (580 ppm) shifts the winning strategy to higher (φ_{RL}) at all the total nitrogen levels. As shown in Fig. 4, the winning strategy shifts from φ_{RL}=5 to φ_{RL}=8 at 114.5 g N m^{-2} and from φ_{RL} =2 to φ_{RL}=4 at 489.5 g N m^{-2}.

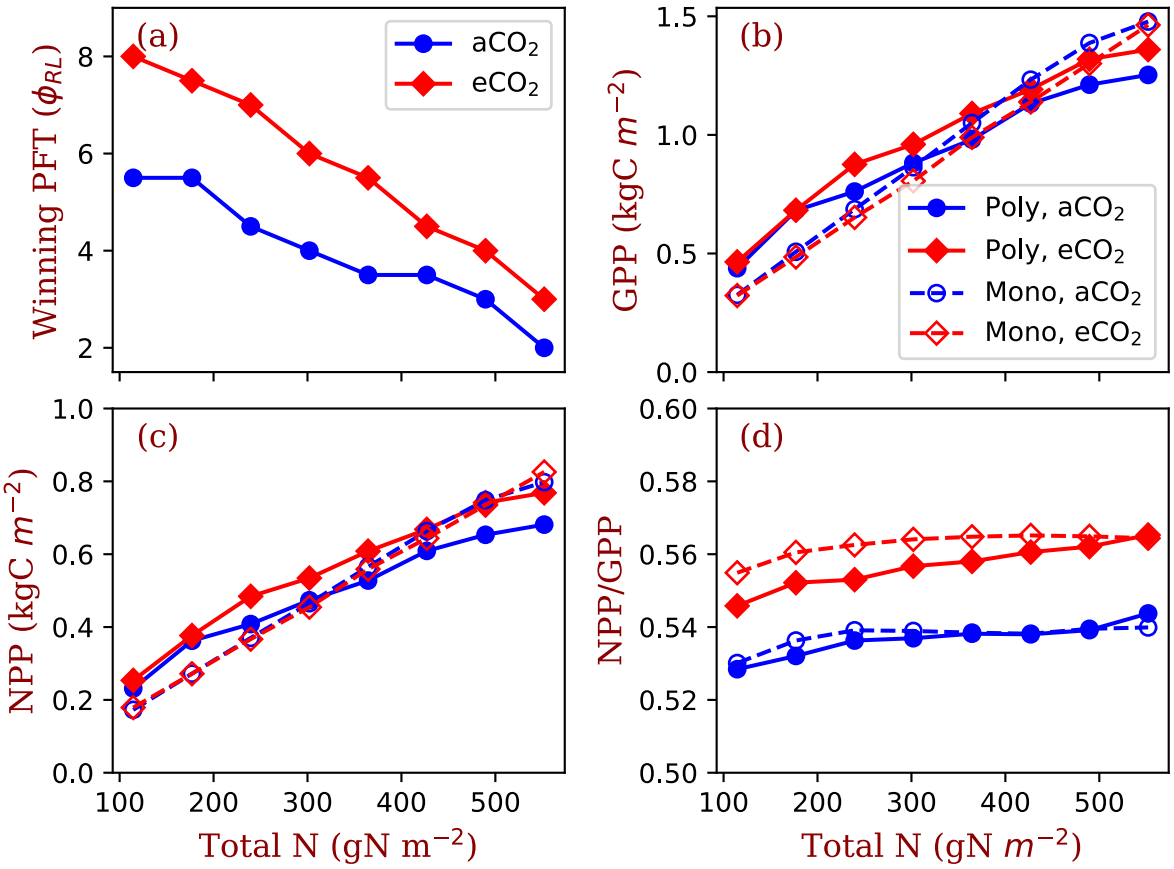

Figure 5 Winning PFTs (φ_{RL}, a) in polyculture runs II and equilibrium Gross Primary Production (GPP, b), Net Primary Production (NPP, c), and Carbon Use Efficiency (NPP/GPP, d). The closed symbols with solid line represent polyculture runs. The open symbols with dashed lines represent monoculture runs (only φ_{RL}=4 shown in this figure).

409 Based on the shifts of the winning φ_{RL} from aCO_2 to eCO_2 at the eight nitrogen levels, we
410 designed the polyculture runs II with high resolution of φ_{RL} and calculated their GPP, NPP,
411 allocation, and plant biomass at equilibrium state. The of φ_{RL} of the winning PFTs decreases
412 from 5.5 to 2 at ambient [CO_2] and from 8.0 to 3.0 at elevated [CO_2] as total N increases from
413 114.5 gN m^{-2} to 552.0 gN m^{-2}. The equilibrium GPP and NPP increase with total nitrogen at
414 values similar to those of the monoculture runs (Fig. 5: b and c). However, the CO_2 stimulation
415 of NPP increases with total nitrogen in the polyculture runs more than it in the monoculture runs.
416 Elevated [CO_2] increases carbon use efficiency (defined as the ratio of NPP to GPP in this study,
417 NPP/GPP) in both the monoculture and polyculture runs (Fig. 5: d). Also, the dependence of
418 NPP:GPP ratio on nitrogen is higher in the polyculture runs than it in the monoculture runs (Fig.
419 5:c).

420 Allocation of NPP to leaves increases with total nitrogen in all conditions, i.e. both
421 competition and monoculture at both ambient [CO_2] and elevated [CO_2] (Fig. 6: a). Foliage NPP
422 is similar in these four model runs when N is low. At high nitrogen (>400 g N m^{-2}), polyculture
423 runs have higher foliage NPP than the monoculture runs generally. Allocation to leaves is
424 relatively stable across the nitrogen gradient at the two CO_2 concentration levels (Fig. 6: b). The
425 fraction of NPP allocated to leaves changes little with nitrogen (Fig. 6: b) and it is universally
426 higher at ambient [CO_2] than at elevated [CO_2].

427

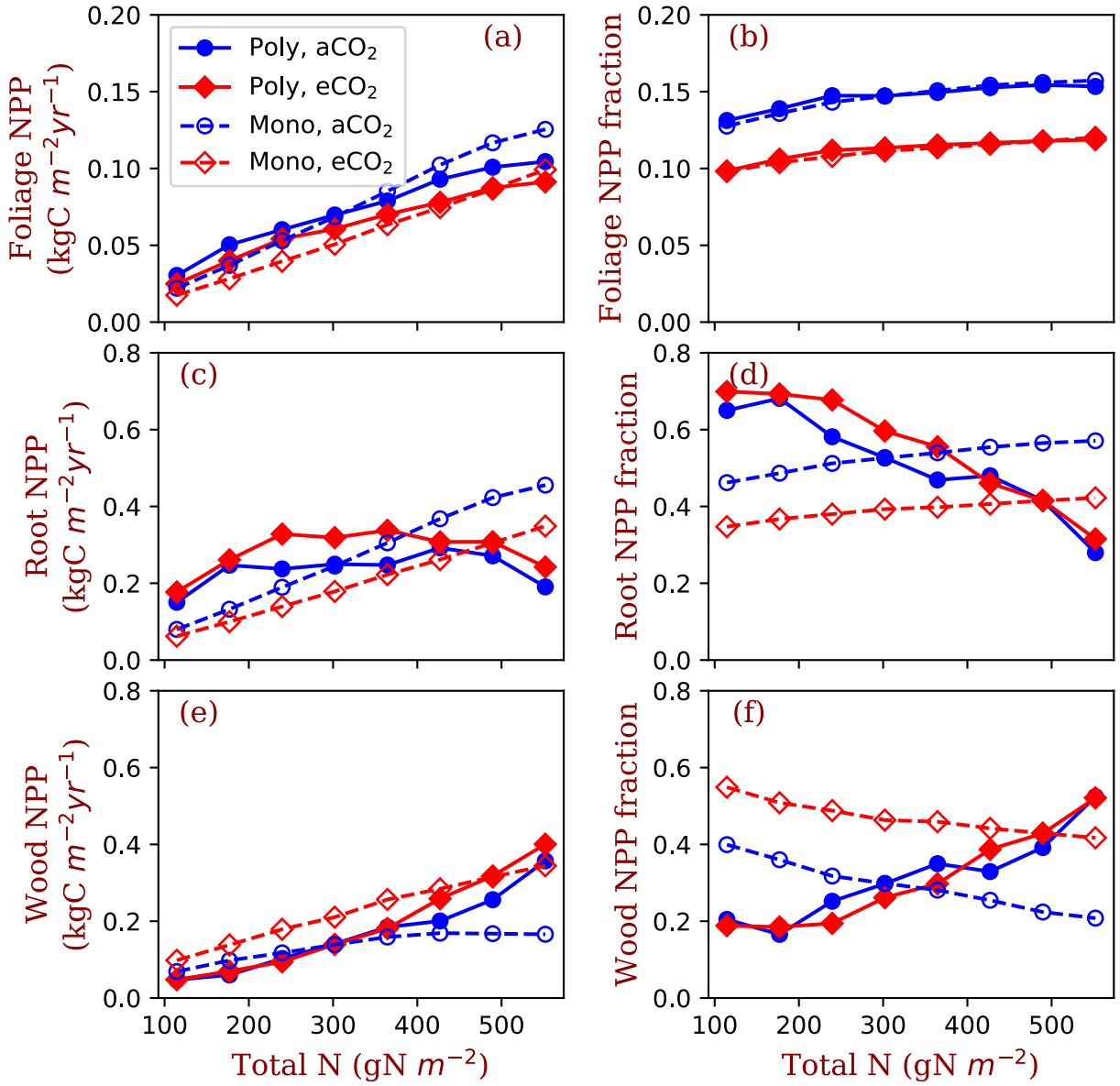

Figure 6 Allocation to leaves, fine roots, and wood tissues of the competition and monoculture runs at the eight total nitrogen levels and two CO_2 concentrations. The panels a, c, and e show the NPP allocated to the tissues and the panels b, d, and f show the fractions of the allocation in total NPP. The closed symbols with solid line represent polyculture runs (poly.). The open symbols with dashed lines represent monoculture runs (only φ_{RL}=4 shown in this figure).

435 Fine root NPP does not significantly change with total nitrogen in polyculture runs,
436 whereas it increases monotonically with increasing nitrogen in monoculture runs (Fig. 6: c).
437 Elevated [CO_2] increases fine root allocation at low nitrogen in polyculture runs but decreases
438 root allocation irrespective of nitrogen in monoculture runs (Fig. 6: c). The fraction of NPP
439 allocated to fine roots decreases with nitrogen at both CO_2 concentrations in polyculture runs but
440 it increases slightly in monoculture runs (Fig. 6: d). In monoculture runs, elevated CO_2 reduces
441 the fraction of NPP allocated to fine roots at all nitrogen levels. In polyculture runs, fractional
442 allocation to fine roots increases at elevated [CO_2] when ecosystem total nitrogen is low (e.g.,
443 114.5 - 302 g N m^{-2}) and decrease at elevated [CO_2] when ecosystem total nitrogen is high (e.g.,
444 364-552 g N m^{-2}).

445 In the reverse of the fine root response, NPP allocation to woody tissues increases with
446 total nitrogen in both competition and monoculture runs (Fig. 6: e). In polyculture runs, the
447 fraction of allocation to woody tissues decreases at elevated [CO_2] when ecosystem total
448 nitrogen is low (e.g., 114 – 245 g N m^{-2}) and increases at elevated [CO_2] when ecosystem total
449 nitrogen is high (e.g., 302 – 552 g N m^{-2}).

450

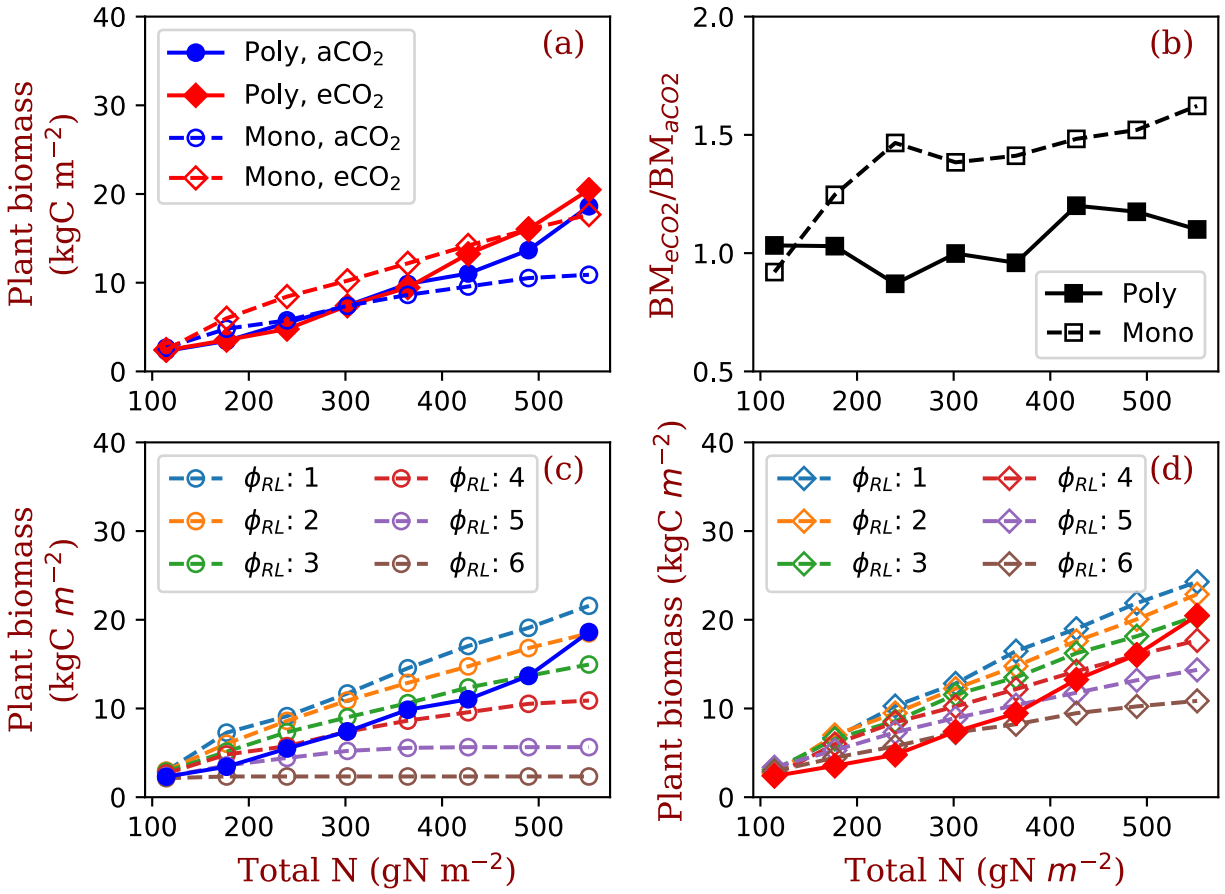

451

452 **Figure 7 Plant biomass responses to elevated [CO_2] and nitrogen**

453 Panel a shows the equilibrium plant biomass (means of simulated plant biomass from model run
454 year 1400 to 1800) in polyculture runs and monoculture runs (φ_{RL}=4). Panel b shows the ratio of
455 simulated plant biomass at elevated [CO_2] to ambient [CO_2] for both competition and
456 monoculture runs. Panels c and d show the comparisons with monoculture runs with φ_{RL}
457 increasing from 1 to 6 at ambient (c) and elevated [CO_2] (d). The closed symbols with solid line
458 represent polyculture runs. The open symbols with dashed lines represent monoculture runs (φ_{RL}
459 ranges from 1 to 6).

460

As a result of the changes in competitively-optimal φ_{RL}, plant biomass increases dramatically with ecosystem nitrogen in polyculture runs compared with that in monoculture runs (Fig. 7: a). The effects of elevated [CO_2] on plant biomass increase with nitrogen in polyculture runs but are constant overall in monoculture runs (Fig. 7: b). Compared with the full spread of monoculture runs with φ_{RL} ranging from 1 to 6, polyculture runs have high root allocation at low nitrogen and low root allocation at high nitrogen due to changes in the dominant competitive allocation strategy, which amplifies plant biomass responses to elevated [CO_2] with increasing nitrogen (Fig. 7: c and d).

4 Discussion

Our competitively-optimal predictions are generally consistent with observations of forest ecosystem production and allocation. For example, high nitrogen environments (i.e., productive environments) favor high wood allocation and low root allocation (Litton et al., 2007; Poorter et al., 2012) because the woody tissues are an unlimited sink for surplus carbon. Low nitrogen availability limits plant CO_2 responses (Norby et al. 2010) in the competition runs (polyculture) because of high root allocation. Our model predicts increased root allocation at all nitrogen levels in response to elevated [CO_2] in the competition runs. Data from free air CO_2 enhancement (FACE) forest experiments largely agree (Drake et al., 2011; Iversen et al., 2012; Jackson et al., 2009; Lukac et al., 2003; Nie et al., 2013; Pritchard et al., 2008; Smith et al., 2013). However, in ORNL-FACE, the increases in root production due to elevated CO_2 increase and then declined after 8 years of CO_2 enhancement (Iversen, 2010; Norby and Zak, 2011). Though there are no direct data available for quantitatively validating the patterns predicted by

483 our model, especially for the long-term, competitive runs, a detailed modeling analysis can help
484 to understand the varied patterns in the experiments and shed light on the modeling of allocation.
485
486 **4.1 Modeling of allocation and competition and their effects on model predictions**
487 In our model, the allocation of carbon and nitrogen within an individual tree is based on
488 allometric scaling, functional relationships, and optimization of resource usage. Basically, the
489 allometric scaling relationships define the maximum leaf and fine root growth at a given tree size
490 and the functional relationships (pipe model) define the ratios of leaf area to sapwood cross-
491 sectional area and fine root surface area. These rules are commonly used in ecosystem models
492 (Franklin et al., 2012) and have been shown to generate reasonable predictions (De Kauwe et al.,
493 2014; Valentine and Mäkelä, 2012). Overall, these rules lead to the priority of allocation to
494 leaves and fine roots but allow for structurally-unlimited stem growth when resources (carbon
495 and nitrogen in this study) are available (i.e., the remainder goes to stems after leaf and fine root
496 growth).
497 We define a maximum leaf and fine root allocation, $f_{LFR,max}$, to limit the maximum
498 allocation to leaves and fine roots to maintain a relatively stable growth rate of wood in years of
499 low productivity. The simulated wood growth patterns agree with real wood growth in temperate
500 trees (Cuny et al., 2012; Michelot et al., 2012). Trees need to grow new wood tissues
501 continuously (especially early in the growing season) to maintain their functions (Plomion et al.,
502 2001). This parameter does not change the fact that leaves and fine roots are the priority. Since
503 allocation ratios to stems are around 0.4~0.7 in temperate forests (Curtis et al., 2002; Litton et
504 al., 2007), with a value of 0.85, $f_{LFR,max}$ only seldom affects the overall carbon allocation ratios of
505 leaves, fine roots, and stems, and still maintains wood grow in years of low productivity. If

506 $f_{LFR,max}$ = 1 (i.e., the highest priority for leaf and fine root growth), simulated trunk radial growth
507 would have unreasonably high interannual variation because leaf and fine root growth would use
508 all carbon to approach to their targets, leaving nothing for stems in some years of low
509 productivity.

510 The simulation of competition for light and soil resources is based on two fundamental
511 mechanisms: 1) competition for light is based on the height of trees according to the rules of the
512 PPA model (Strigul et al., 2008); and 2) individual nitrogen uptake is linearly dependent on the
513 fine root surface area of an individual tree relative to that of its neighbors (Dybzinski et al., 2019;
514 McMurtrie et al., 2012; Weng et al., 2017). These two mechanisms define an allocational
515 tradeoff between wood and fine roots for carbon and nitrogen investment in different [CO_2] and
516 nitrogen environments. Allowing competition for these resources to determine the dominant
517 traits results in very different predicted allocation patterns – and thus ecosystem level responses
518 – than those of fixed allocation strategies. For example, fractional wood allocation increases with
519 increasing nitrogen availability under competitive allocation but decreases – the opposite
520 qualitative response – under a fixed strategy (Fig. 6: f). Consequently, equilibrium plant biomass
521 is predicted to increase much more with increasing nitrogen availability under a competitive
522 strategy than under a fixed strategy (Fig. 4: c, d). In nature, the effects of competition on
523 dominant plant traits may occur through species replacement or community assembly (akin to
524 the mechanism in our model), but it may also occur through adaptive plastic responses or in-
525 place sub-population evolution of ecotypes.

526 Although the strategy that maximizes the growth rate in a fixed-allocation strategy
527 allocates very little to fine roots (Figs. 3 and S1), the competitively optimal strategy allocates
528 more carbon to fine roots to compete for nitrogen, a competitive effect termed “fine-root

529 overproliferation" (Gersani et al., 2001; McNickle and Dybzinski, 2013; O'Brien et al., 2005).
530 Elevated [CO_2] increases the carbon gain of leaves, making more carbon available for roots to
531 compete for nitrogen and thus exacerbating the fine-root overproliferation (Dybzinski et al.,
532 2015). Because most nitrogen uptake is via mass flow and diffusion (Oyewole et al., 2017) and
533 because both of these mechanisms depend on sink strength, individuals with *relatively* greater
534 fine root mass than their neighbors take a greater share of nitrogen, as was recently demonstrated
535 empirically (Dybzinski et al., 2019; Kulmatiski et al., 2017). Thus, fine roots may overproliferate
536 for competitive reasons relative to lower optimal fine root mass in the hypothetical absence of an
537 evolutionary history of competition (Craine, 2006; McNickle and Dybzinski, 2013). The
538 increased fitness (*i.e.*, reproductive success) of the *relatively* greater strategy increases the
539 *absolute* fine root mass. But again, individuals with even *relatively* greater fine root mass take a
540 greater share of nitrogen, leading to what has been termed a "tragedy of the commons" (Gersani
541 et al., 2001). This may also explain why root C:N ratio is highly variable (Dybzinski et al., 2015;
542 Luo et al., 2006; Nie et al., 2013): a high density of fine roots in soil may be more important than
543 the high absorption ability of a single root in competing for soil nitrogen in the usually low
544 mineral nitrogen soils.

545 Root overproliferation is still controversial in experiments. For example, Gersani et al.
546 (2001) and O'Brien (2005) found competing plants generate more roots than those planted
547 isolated for pea and soybeans, respectively; whereas, McNickle and Brown (2014) found root
548 growth follows the availability of soil nutrients and individuals growth with competitors have the
549 same root growth as that predicted by the changed nutrient availability. Roots are far more
550 adaptive and complex than those simulated in models at modifying their growth patterns in
551 response to soil nutrient and water dynamics (Hodge, 2009). The root growth strategies in

552 response to competition also vary with species (Belter and Cahill, 2015). The mechanisms of
553 self-recognition of inter- and intra- roots also can lead to varied behavior of root growth (Chen et
554 al., 2012). However, all of the aforementioned studies considered only *plastic* root
555 overproliferation, where individuals produce more roots in the presence of other individuals than
556 they do in isolation, analogous to stem elongation of crowded seedlings (Dudley and Schmitt,
557 1996). A portion of root overproliferation may also be *fixed*, analogous to trees that still grow tall
558 even when grown in isolation. Dybzinski et al. (2019) showed that plant community nitrogen
559 uptake rate was independent of fine root mass in seedlings of numerous species, suggesting a
560 high degree of fixed fine root overproliferation. To improve root competition models, more
561 detailed experiments that control root growth should be conducted to quantify the marginal
562 benefits of roots in isolated, monoculture, and polyculture environments.

563 At high soil nitrogen, height-structured competition for light (also a game-theoretic
564 tragedy of the commons, Falster and Westoby, 2003; Givnish, 1982) prevails, and trees with
565 greater *relative* allocation to trunks prevail. The balance between these two competitive
566 priorities (fine roots vs. stems) can be observed in our model predictions as a shift from fine root
567 allocation to wood allocation as soil nitrogen increases. The increases in the critical height,
568 which is the height of the shortest tree in canopy layer, from low nitrogen to high nitrogen
569 indicates a shift from the importance of competition for soil nitrogen to the importance of
570 competition for light as ecosystem nitrogen increases (Fig. S6). Because the most competitive
571 type shifts from high fine root allocation to low fine root allocation as ecosystem total nitrogen
572 increases, increases in NPP and plant biomass across the nitrogen gradient are greater than the
573 increases in NPP and plant biomass under the fixed strategy (Fig. 3). This greatly reduces the
574 carbon cost of belowground competition. The slight decrease in the fraction of NPP allocated to

575 leaves at elevated [CO_2] occurs because of increases in total NPP and constant absolute NPP
576 allocation to foliage. It is consistent with FACE experiments that show leaf area index (LAI) in
577 closed-canopy forests is not responsive to elevated [CO_2] (Norby et al., 2003).

578 Our model predicts that the ratio of plant biomass under elevated [CO_2] relative to plant
579 biomass under ambient [CO_2] should increase with increasing nitrogen due to the shift of carbon
580 allocation from fine roots to woody tissues. In contrast, the analytic model of Dybzinski *et al*.
581 (2015) predicts that the ratio of plant biomass under elevated [CO_2] relative to plant biomass
582 under ambient [CO_2] should be largely independent of total nitrogen because of an increasing
583 shift in carbon allocation from long-lived, low-nitrogen wood to short-lived, high-nitrogen fine
584 roots under elevated [CO_2] and with increasing nitrogen. This significant difference between
585 these two predictions traces back to differences in how fine root stoichiometry is handled in the
586 two models. In the model of Dybzinski *et al*. (2015), the fine root C:N ratio is flexible and the
587 marginal nitrogen uptake capacity per unit of carbon allocated to fine roots depends on its
588 nitrogen concentration. Like the model presented here, the model of Dybzinski *et al*. (2015)
589 predicts decreasing fine root mass with increasing nitrogen availability. *Unlike* the model
590 presented here (which has constant fine root nitrogen concentration), the model of Dybzinski et
591 al. (2015) predicts increasing fine root nitrogen concentration with increasing nitrogen
592 availability. As a result, there is less nitrogen to allocate to wood as nitrogen increases in the
593 model of Dybzinski *et al*. (2015) than there is in the model presented here. These countervailing
594 factors even out the ratio of plant biomass under elevated [CO_2] relative to plant biomass under
595 ambient [CO_2] across the nitrogen gradient in Dybzinski *et al*. (2015), whereas their absence
596 amplifies this ratio with increasing nitrogen in the model presented here. Our ability to diagnose

and understand this discrepancy highlights the utility of deploying closely-related analytical and simulation models (Weng et al., 2017).

4.2 Model complexity and uncertainty

Compared with the conventional pool-based vegetation models that use pools and fluxes to represent plant demographic processes at a land simulation unit (e.g., grid or patch), VDMs add two more layers of complexity. The first is the inclusion of stochastic birth and mortality processes of individuals (i.e., demographic processes). These processes allow the models to predict population dynamics and transient vegetation structure, such as size-structured distribution and crown organization (e.g., Moorcroft et al., 2001; Strigul et al., 2008). With changes in vegetation structure, allocation and mortality rates can change, generating a different carbon storage accumulation curve compared with those predicted by pool-based models where vegetation structure is not explicitly represented (e.g., Weng et al., 2015). The second is the simulated shift in dominant plant traits during succession due to the shifting of competitive outcomes among different PFTs, which changes the allocation between fast- and slow-turnover pools and thus the parameters of allocation and the residence time of carbon in the ecosystem.

Together, these mechanisms may alter long-term predictions of terrestrial carbon cycling due to changes in PFT-based parameters (Dybzinski et al., 2011; Farrior et al., 2013; Weng et al., 2015). As described in the Introduction, current pool-based models can be described by a linear system of equations characterized by the key parameters of allocation, residence time, and transfer coefficients (Eq. 1) with the rigid assumption of unchangeable plant types (Luo et al., 2012; Xia et al., 2013). In VDMs however, allocation, residence time, leaf traits, phenology, mortality, plant forms, and their responses to climate change are all strategies of competition whose success varies with the environmental conditions and the traits of the individuals they are

620 competing against. To make predictions of carbon cycle responses to the novel conditions of
621 climate change, we must understand what determines the most competitive strategy, how the
622 most competitive strategy changes with conditions, and how the most competitive strategy
623 impacts the carbon cycle.

624 Many trade-offs between plant traits can shift in response to environmental and biotic
625 changes, limiting the applicability of varying a single trait, as we have in this study. For example,
626 allocation, leaf traits, mycorrhizal types, and nitrogen fixation can all change with ecosystem
627 nitrogen availability (Menge et al., 2017; Ordoñez et al., 2009; Phillips et al., 2013; Vitousek et
628 al., 2013). The unrealistic effects of model simplification can be corrected by adding important
629 tradeoffs that are missing. For example, the positive feedback between root allocation and SOM
630 decomposition plays a role in mitigating the effects of tragedies of the commons of root over-
631 proliferation (e.g., Gersani et al., 2001; Zea-Cabrera et al., 2006) due to a negative feedback
632 induced by root turnover. High root allocation increases the decomposition rate of SOM and the
633 supply of mineral nitrogen because of the high turnover rate of root litter, which favors a strategy
634 of high wood allocation and reduces the competitive optimal fine root allocation. This negative
635 feedback indicates that the model structure is flexible and that we can incorporate correct
636 mechanisms step by step to improve model prediction skills. Testing single strategies is still a
637 necessary step to improving our understanding of the system and prediction skills of the models,
638 though it could lead to unrealistic responses sometimes.
639

640 **4.3 Implications for Earth system modeling**

641 As shown in model inter-comparison studies, the mechanisms of modeling allocation
642 differ very much, leading to high variation in their predictions (e.g., De Kauwe et al. 2014).

643 Calibrating model parameters to fit data may not increase model predictive skill because data are
644 often also highly variable. Franklin et al. (2012) suggest that in order to build realistic and
645 predictive allocation models, we should correctly identify and implement fundamental principles.
646 Our model predicts similar patterns to those of Valentine and Mäkelä (2012), which are very
647 different in their details but share fundamental principles, including 1) evolutionary- or
648 competitive-optimization, 2) capped leaves and fine roots, 3) structurally unlimited stem
649 allocation (i.e., for optimizing carbon use), and 4) height-structure competition for light and root-
650 mass-based competition for soil resources. The principles 2 and 3 are commonly used in models
651 (De Kauwe et al., 2014; Jiang et al., 2019). However, the different rules of implementing them
652 (e.g., allometric equation, functional relationships, etc.) lead to highly varied predictions (as
653 shown in De Kauwe et al., 2014), though the formulations may be very similar. In competitively-
654 optimal models, such as this study and also Valentine and Mäkelä (2012), the competition
655 processes generate similar emergent patterns by selecting those that can survive in competition,
656 regardless the details of those differences.

657 In this study, similar as in Valentine and Mäkelä (2012), there is a hypothesis for the
658 tradeoffs between light capture and nitrogen uptake via allocation based on insights gained from
659 simpler models (e.g., Dybzinski et al., 2015; Mäkelä et al., 2008) for predicting allocation as an
660 emergent property of competition. One advantage of building a model in this way is that the
661 vegetation dynamics are predicted from first principles, rather than based on the correlations
662 between vegetation properties and environmental conditions. With these first principles, the
663 models can produce reasonable predictions, though the details of physiological and demographic
664 processes vary among models. For vegetation models designed to predict the effects of climate
665 change, the important operational distinction is that the fundamental rules cannot or will not

666 change as climate changes. Nor, presumably, will the underlying ecological and evolutionary
667 processes change as climate changes. The emergent properties can change as climate changes
668 however, and the models built on the "scale-appropriate" unbreakable constraints and ecological
669 and evolutionary processes will be able to accurately predict changes in emergent ecosystem
670 properties.

671 This modeling approach also demands improvement in model validation and benchmarking
672 systems (Collier et al., 2018; Hoffman et al., 2017). As shown in this study, allocation responses
673 to elevated CO_2 at different nitrogen levels in monoculture runs are opposite to those in
674 competitive-allocation runs. For example, in monoculture runs, elevated [CO_2] increases wood
675 allocation and decreases fine root allocation at low nitrogen; whereas in competitive-allocation
676 runs elevated [CO_2] leads to low wood allocation and high fine root allocation. Simply
677 calibrating against short-term observational data may improve the agreements with observations
678 but would not change model predictions because these results emerge from the fundamental
679 assumptions of the models. An updated model benchmarking system should have the metrics of
680 competitive plant traits during the development of ecosystems and their responses to changes in
681 climate.

682

683 **5 Conclusions**

684 Our study illustrates that including the competition processes for light and soil resources in
685 a game-theoretic vegetation demographic model can substantially change the prediction of the
686 contribution of ecosystems to the global carbon cycle. Allowing the model to track the
687 competitive allocation strategies can generate significantly different ecosystem-level predictions
688 (e.g., biomass and ecosystem carbon storage) than those of fixed strategies. Building such a

model requires differentiating between the unbreakable tradeoffs of plant traits and ecological processes from the emergent properties of ecosystems. Drawing on insights from closely-related analytical models to develop and understand more complicated simulation models seems, to us, indispensable. Evaluating these models also requires an updated model benchmarking system that includes the metrics of competitive plant traits during the development of ecosystems and their responses to climate changes.

Acknowledgements

This work was supported by NASA Modeling, Analysis, and Prediction (MAP) Program (NNH16ZDA001N-MAP), USDA Forest Service Northern Research Station (Agreement 13-JV-11242315-066) and Princeton Environment Institute. C.E.F acknowledges support from the University of Texas at Austin.

Codes and data availability

The codes of the BiomeE model are available at GitHub:

https://github.com/wengensheng/BiomeESS

The simulated data from simulation experiments and Python scripts used in this study will be made publicly available at the publish of this paper.

Reference

Aber, J. D., Magill, A., Boone, R., Melillo, J. M. and Steudler, P.: Plant and Soil Responses to Chronic Nitrogen Additions at the Harvard Forest, Massachusetts, Ecological Applications, 3(1), 156–166, doi:10.2307/1941798, 1993.

Arora, V. K. and Boer, G. J.: A parameterization of leaf phenology for the terrestrial ecosystem component of climate models, Global Change Biology, 11(1), 39–59, doi:10.1111/j.1365-2486.2004.00890.x, 2005.

Barr, A. G., Ricciu, D. M., Schaefer, K., Richarson, A., Agarwal, D., Thornton, P. E., Davis, K., Jackson, B., Cook, R. B., Hollinger, D. Y., Van Ingen, C., Amiro, B., Andrews, A., Arain, M. A., Baldocchi, D., Black, T. A., Bolstad, P., Curtis, P., Desai, A., Dragoni, D., Flanagan, L., Gu, L., Katul, G., Law, B. E., Lafleur, P. M., Margolis, H., Matamala, R., Meyers, T., McCaughey, J. H., Monson, R., Munger, J. W., Oechel, W., Oren, R., Roulet, N. T., Torn, M. and Verma, S. B.: NACP Site: Tower Meteorology, Flux Observations with Uncertainty, and Ancillary Data, , doi:10.3334/ornldaac/1178, 2013.

Belter, P. R. and Cahill, J. F.: Disentangling root system responses to neighbours: identification of novel root behavioural strategies, AoB PLANTS, 7, plv059, doi:10.1093/aobpla/plv059, 2015.

Bloom, A. A., Exbrayat, J.-F., van der Velde, I. R., Feng, L. and Williams, M.: The decadal state of the terrestrial carbon cycle: Global retrievals of terrestrial carbon allocation, pools, and residence times, Proceedings of the National Academy of Sciences, 113(5), 1285–1290, doi:10.1073/pnas.1515160113, 2016.

Cannell, M. G. R. and Dewar, R. C.: Carbon Allocation in Trees: a Review of Concepts for Modelling, in Advances in Ecological Research, vol. 25, pp. 59–104, Elsevier., 1994.

Chen, B. J. W., During, H. J. and Anten, N. P. R.: Detect thy neighbor: Identity recognition at the root level in plants, Plant Science, 195, 157–167, doi:10.1016/j.plantsci.2012.07.006, 2012.

Collier, N., Hoffman, F. M., Lawrence, D. M., Keppel-Aleks, G., Koven, C. D., Riley, W. J., Mu, M. and Randerson, J. T.: The International Land Model Benchmarking (ILAMB) System: Design, Theory, and Implementation, Journal of Advances in Modeling Earth Systems, 10(11), 2731–2754, doi:10.1029/2018MS001354, 2018.

Compton, J. E. and Boone, R. D.: Long-Term Impacts of Agriculture on Soil Carbon and Nitrogen in New England Forests, Ecology, 81(8), 2314, doi:10.2307/177117, 2000.

Craine, J. M.: Competition for Nutrients and Optimal Root Allocation, Plant and Soil, 285(1–2), 171–185, doi:10.1007/s11104-006-9002-x, 2006.

Cuny, H. E., Rathgeber, C. B. K., Lebourgeois, F., Fortin, M. and Fournier, M.: Life strategies in intra-annual dynamics of wood formation: example of three conifer species in a temperate forest in north-east France, Tree Physiology, 32(5), 612–625, doi:10.1093/treephys/tps039, 2012.

Curtis, P. S., Hanson, P. J., Bolstad, P., Barford, C., Randolph, J. ., Schmid, H. . and Wilson, K. B.: Biometric and eddy-covariance based estimates of annual carbon storage in five eastern North American deciduous forests, Agricultural and Forest Meteorology, 113(1–4), 3–19, doi:10.1016/S0168-1923(02)00099-0, 2002.

De Kauwe, M. G., Medlyn, B. E., Zaehle, S., Walker, A. P., Dietze, M. C., Wang, Y.-P., Luo, Y., Jain, A. K., El-Masri, B., Hickler, T., Wårlind, D., Weng, E., Parton, W. J., Thornton, P. E., Wang, S., Prentice, I. C., Asao, S., Smith, B., McCarthy, H. R., Iversen, C. M., Hanson, P. J., Warren, J. M., Oren, R. and Norby, R. J.: Where does the carbon go? A model-data intercomparison of vegetation carbon allocation and turnover processes at two temperate forest free-air CO_2 enrichment sites, New Phytologist, 203(3), 883–899, doi:10.1111/nph.12847, 2014.

DeAngelis, D. L., Ju, S., Liu, R., Bryant, J. P. and Gourley, S. A.: Plant allocation of carbon to defense as a function of herbivory, light and nutrient availability, Theoretical Ecology, 5(3), 445–456, doi:10.1007/s12080-011-0135-z, 2012.

Drake, J. E., Gallet-Budynek, A., Hofmockel, K. S., Bernhardt, E. S., Billings, S. A., Jackson, R. B., Johnsen, K. S., Lichter, J., McCarthy, H. R., McCormack, M. L., Moore, D. J. P., Oren, R., Palmroth, S., Phillips, R. P., Pippen, J. S., Pritchard, S. G., Treseder, K. K., Schlesinger, W. H., DeLucia, E. H. and Finzi, A. C.: Increases in the flux of carbon belowground stimulate nitrogen uptake and sustain the long-term enhancement of forest productivity under elevated CO2, ECOLOGY LETTERS, 14(4), 349–357, doi:10.1111/j.1461-0248.2011.01593.x, 2011.

Dudley, S. A. and Schmitt, J.: Testing the adaptive plasticity hypothesis: density-dependent selection on manipulated stem length in Impatiens capensis, The American Naturalist, 147(3), 445–465, doi:10.1086/285860, 1996.

Dybzinski, R., Farrior, C., Wolf, A., Reich, P. B. and Pacala, S. W.: Evolutionarily Stable Strategy Carbon Allocation to Foliage, Wood, and Fine Roots in Trees Competing for Light and Nitrogen: An Analytically Tractable, Individual-Based Model and Quantitative Comparisons to Data, American Naturalist, 177(2), 153–166, doi:10.1086/657992, 2011.

Dybzinski, R., Farrior, C. E. and Pacala, S. W.: Increased forest carbon storage with increased atmospheric CO2 despite nitrogen limitation: a game-theoretic allocation model for trees in competition for nitrogen and light, Global Change Biology, 21(3), 1182–1196, doi:10.1111/gcb.12783, 2015.

Dybzinski, R., Kelvakis, A., McCabe, J., Panock, S., Anuchitlertchon, K., Vasarhelyi, L., Luke McCormack, M., McNickle, G. G., Poorter, H., Trinder, C. and Farrior, C. E.: How are nitrogen availability, fine-root mass, and nitrogen uptake related empirically? Implications for models and theory, Global Change Biology, doi:10.1111/gcb.14541, 2019.

Emanuel, W. R. and Killough, G. G.: Modeling terrestrial ecosystems in the global carbon cycle with Shifts in carbon storage capacity by land-use change, Ecology, 65(3), 970–983, doi:10.2307/1938069, 1984.

Eriksson, E.: Compartment Models and Reservoir Theory, Annual Review of Ecology and Systematics, 2(1), 67–84, doi:10.1146/annurev.es.02.110171.000435, 1971.

Falster, D. and Westoby, M.: Plant height and evolutionary games, TRENDS IN ECOLOGY & EVOLUTION, 18(7), 337–343, doi:10.1016/S0169-5347(03)00061-2, 2003.

Farrior, C. E., Dybzinski, R., Levin, S. A. and Pacala, S. W.: Competition for Water and Light in Closed-Canopy Forests: A Tractable Model of Carbon Allocation with Implications for Carbon Sinks, American Naturalist, 181(3), 314–330, doi:10.1086/669153, 2013.

Farrior, C. E., Rodriguez-Iturbe, I., Dybzinski, R., Levin, S. A. and Pacala, S. W.: Decreased water limitation under elevated CO2 amplifies potential for forest carbon sinks, Proceedings of the National Academy of Sciences of the United States of America, 112(23), 7213–7218, doi:10.1073/pnas.1506262112, 2015.

Fisher, R. A., Koven, C. D., Anderegg, W. R. L., Christoffersen, B. O., Dietze, M. C., Farrior, C. E., Holm, J. A., Hurtt, G. C., Knox, R. G., Lawrence, P. J., Lichstein, J. W., Longo, M., Matheny, A. M., Medvigy, D., Muller-Landau, H. C., Powell, T. L., Serbin, S. P., Sato, H., Shuman, J. K., Smith, B., Trugman, A. T., Viskari, T., Verbeeck, H., Weng, E., Xu, C., Xu, X., Zhang, T. and Moorcroft, P. R.: Vegetation demographics in Earth System Models: A review of progress and priorities, Global Change Biology, 24(1), 35–54, doi:10.1111/gcb.13910, 2018.

Franklin, O., Johansson, J., Dewar, R. C., Dieckmann, U., McMurtrie, R. E., Brannstrom, A. and Dybzinski, R.: Modeling carbon allocation in trees: a search for principles, Tree Physiology, 32(6), 648–666, doi:10.1093/treephys/tpr138, 2012.

Friend, A. D., Arneth, A., Kiang, N. Y., Lomas, M., Ogee, J., Roedenbeckk, C., Running, S. W., Santaren, J.-D., Sitch, S., Viovy, N., Woodward, F. I. and Zaehle, S.: FLUXNET and modelling the global carbon cycle, Global Change Biology, 13(3), 610–633, doi:10.1111/j.1365-2486.2006.01223.x, 2007.

Gersani, M., Brown, J. s., O'Brien, E. E., Maina, G. M. and Abramsky, Z.: Tragedy of the commons as a result of root competition, Journal of Ecology, 89(4), 660–669, doi:10.1046/j.0022-0477.2001.00609.x, 2001.

Givnish, T. J.: On the Adaptive Significance of Leaf Height in Forest Herbs, The American Naturalist, 120(3), 353–381, doi:10.1086/283995, 1982.

Haverd, V., Smith, B., Raupach, M., Briggs, P., Nieradzik, L., Beringer, J., Hutley, L., Trudinger, C. M. and Cleverly, J.: Coupling carbon allocation with leaf and root phenology predicts tree–grass partitioning along a savanna rainfall gradient, Biogeosciences, 13(3), 761–779, doi:10.5194/bg-13-761-2016, 2016.

Hibbs, D. E.: Forty Years of Forest Succession in Central New England, Ecology, 64(6), 1394–1401, doi:10.2307/1937493, 1983.

Hodge, A.: Root decisions, Plant, Cell & Environment, 32(6), 628–640, doi:10.1111/j.1365-3040.2008.01891.x, 2009.

Hoffman, F. M., Koven, C. D., Keppel-Aleks, G., Lawrence, D. M., Riley, W. J., Randerson, J. T., Ahlström, A., Abramowitz, G., Baldocchi, D. D., Best, M. J., Bond-Lamberty, B., De Kauwe, M. G., Denning, A. S., Desai, A. R., Eyring, V., Fisher, J. B., Fisher, R. A., Gleckler, P. J., Huang, M., Hugelius, G., Jain, A. K., Kiang, N. Y., Kim, H., Koster, R. D., Kumar, S. V., Li, H., Luo, Y., Mao, J., McDowell, N. G., Mishra, U., Moorcroft, P. R., Pau, G. S. H., Ricciuto, D. M., Schaefer, K., Schwalm, C. R., Serbin, S. P., Shevliakova, E., Slater, A. G., Tang, J., Williams, M., Xia, J., Xu, C., Joseph, R. and Koch, D.: 2016 International Land Model Benchmarking (ILAMB) Workshop Report., 2017.

Iversen, C. M.: Digging deeper: fine-root responses to rising atmospheric CO2 concentration in forested ecosystems, New Phytologist, 186(2), 346–357, doi:10.1111/j.1469-8137.2009.03122.x, 2010.

Iversen, C. M., Keller, J. K., Garten, C. T. and Norby, R. J.: Soil carbon and nitrogen cycling and storage throughout the soil profile in a sweetgum plantation after 11 years of CO2-enrichment, Global Change Biology, 18(5), 1684–1697, doi:10.1111/j.1365-2486.2012.02643.x, 2012.

Jackson, R. B., Cook, C. W., Pippen, J. S. and Palmer, S. M.: Increased belowground biomass and soil CO_2 fluxes after a decade of carbon dioxide enrichment in a warm-temperate forest, Ecology, 90(12), 3352–3366, doi:10.1890/08-1609.1, 2009.

Jiang, M., Zaehle, S., De Kauwe, M. G., Walker, A. P., Caldararu, S., Ellsworth, D. S. and Medlyn, B. E.: The quasi-equilibrium framework revisited: analyzing long-term CO2 enrichment responses in plant–soil models, Geosci. Model Dev., 12(5), 2069–2089, doi:10.5194/gmd-12-2069-2019, 2019.

Keenan, T. F., Davidson, E. A., Munger, J. W. and Richardson, A. D.: Rate my data: quantifying the value of ecological data for the development of models of the terrestrial carbon cycle, Ecological Applications, 23(1), 273–286, doi:10.1890/12-0747.1, 2013.

Koven, C. D., Chambers, J. Q., Georgiou, K., Knox, R., Negron-Juarez, R., Riley, W. J., Arora, V. K., Brovkin, V., Friedlingstein, P. and Jones, C. D.: Controls on terrestrial carbon feedbacks by productivity versus turnover in the CMIP5 Earth System Models, Biogeosciences, 12(17), 5211–5228, doi:10.5194/bg-12-5211-2015, 2015.

Krinner, G., Viovy, N., de Noblet-Ducoudré, N., Ogée, J., Polcher, J., Friedlingstein, P., Ciais, P., Sitch, S. and Prentice, I. C.: A dynamic global vegetation model for studies of the coupled atmosphere-biosphere system, Global Biogeochemical Cycles, 19(1), doi:10.1029/2003GB002199, 2005.

Kulmatiski, A., Adler, P. B., Stark, J. M. and Tredennick, A. T.: Water and nitrogen uptake are better associated with resource availability than root biomass, Ecosphere, 8(3), e01738, doi:10.1002/ecs2.1738, 2017.

Lacointe, A.: Carbon allocation among tree organs: A review of basic processes and representation in functional-structural tree models, Annals of Forest Science, 57(5), 521–533, doi:10.1051/forest:2000139, 2000.

Leuning, R., Kelliher, F. M., Pury, D. G. G. and Schulze, E.-D.: Leaf nitrogen, photosynthesis, conductance and transpiration: scaling from leaves to canopies, Plant Cell Environ, 18(10), 1183–1200, doi:10.1111/j.1365-3040.1995.tb00628.x, 1995.

Litton, C. M., Raich, J. W. and Ryan, M. G.: Carbon allocation in forest ecosystems, Global Change Biol, 13(10), 2089–2109, doi:10.1111/j.1365-2486.2007.01420.x, 2007.

Lukac, M., Calfapietra, C. and Godbold, D. L.: Production, turnover and mycorrhizal colonization of root systems of three Populus species grown under elevated CO2 (POPFACE), Global Change Biol, 9(6), 838–848, doi:10.1046/j.1365-2486.2003.00582.x, 2003.

Luo, Y. and Weng, E.: Dynamic disequilibrium of the terrestrial carbon cycle under global change, Trends in Ecology & Evolution, 26(2), 96–104, doi:10.1016/j.tree.2010.11.003, 2011.

Luo, Y., Hui, D. and Zhang, D.: Elevated CO2 stimulates net accumulations of carbon and nitrogen in land ecosystems: a meta-analysis, Ecology, 87(1), 53–63, 2006.

Luo, Y. Q., Wu, L. H., Andrews, J. A., White, L., Matamala, R., Schafer, K. V. R. and Schlesinger, W. H.: Elevated CO2 differentiates ecosystem carbon processes: Deconvolution analysis of Duke Forest FACE data, Ecological Monographs, 71(3), 357–376, doi:10.1890/0012-9615(2001)071[0357:ECDECP]2.0.CO;2, 2001.

Luo, Y. Q., Randerson, J. T., Abramowitz, G., Bacour, C., Blyth, E., Carvalhais, N., Ciais, P., Dalmonech, D., Fisher, J. B., Fisher, R., Friedlingstein, P., Hibbard, K., Hoffman, F., Huntzinger, D., Jones, C. D., Koven, C., Lawrence, D., Li, D. J., Mahecha, M., Niu, S. L., Norby, R., Piao, S. L., Qi, X., Peylin, P., Prentice, I. C., Riley, W., Reichstein, M., Schwalm, C., Wang, Y. P., Xia, J. Y., Zaehle, S. and Zhou, X. H.: A framework for benchmarking land models, Biogeosciences, 9(10), 3857–3874, doi:10.5194/bg-9-3857-2012, 2012.

Mäkelä, A., Valentine, H. T. and Helmisaari, H.-S.: Optimal co-allocation of carbon and nitrogen in a forest stand at steady state, New Phytologist, 180(1), 114–123, doi:10.1111/j.1469-8137.2008.02558.x, 2008.

McGill, B. J. and Brown, J. S.: Evolutionary Game Theory and Adaptive Dynamics of Continuous Traits, Annual Review of Ecology, Evolution, and Systematics, 38(1), 403–435, doi:10.1146/annurev.ecolsys.36.091704.175517, 2007.

McMurtrie, R. E., Iversen, C. M., Dewar, R. C., Medlyn, B. E., Näsholm, T., Pepper, D. A. and Norby, R. J.: Plant root distributions and nitrogen uptake predicted by a hypothesis of optimal root foraging, Ecology and Evolution, 2(6), 1235–1250, doi:10.1002/ece3.266, 2012.

McNickle, G. G. and Brown, J. S.: An ideal free distribution explains the root production of plants that do not engage in a tragedy of the commons game, edited by S. Schwinning, Journal of Ecology, 102(4), 963–971, doi:10.1111/1365-2745.12259, 2014.

McNickle, G. G. and Dybzinski, R.: Game theory and plant ecology, edited by J. Klironomos, Ecology Letters, 16(4), 545–555, doi:10.1111/ele.12071, 2013.

Melillo, J. M., Butler, S., Johnson, J., Mohan, J., Steudler, P., Lux, H., Burrows, E., Bowles, F., Smith, R., Scott, L., Vario, C., Hill, T., Burton, A., Zhou, Y.-M. and Tang, J.: Soil warming, carbon-nitrogen interactions, and forest carbon budgets, Proceedings of the National Academy of Sciences, 108(23), 9508–9512, doi:10.1073/pnas.1018189108, 2011.

Menge, D. N. L., Batterman, S. A., Hedin, L. O., Liao, W., Pacala, S. W. and Taylor, B. N.: Why are nitrogen-fixing trees rare at higher compared to lower latitudes?, Ecology, 98(12), 3127–3140, doi:10.1002/ecy.2034, 2017.

Michelot, A., Simard, S., Rathgeber, C., Dufrene, E. and Damesin, C.: Comparing the intra-annual wood formation of three European species (Fagus sylvatica, Quercus petraea and Pinus sylvestris) as related to leaf phenology and non-structural carbohydrate dynamics, Tree Physiology, 32(8), 1033–1045, doi:10.1093/treephys/tps052, 2012.

Montané, F., Fox, A. M., Arellano, A. F., MacBean, N., Alexander, M. R., Dye, A., Bishop, D. A., Trouet, V., Babst, F., Hessl, A. E., Pederson, N., Blanken, P. D., Bohrer, G., Gough, C. M., Litvak, M. E., Novick, K. A., Phillips, R. P., Wood, J. D. and Moore, D. J. P.: Evaluating the effect of alternative carbon allocation schemes in a land surface model (CLM4.5) on carbon fluxes, pools, and turnover in temperate forests, Geoscientific Model Development, 10(9), 3499–3517, doi:10.5194/gmd-10-3499-2017, 2017.

Moorcroft, P. R., Hurtt, G. C. and Pacala, S. W.: A method for scaling vegetation dynamics: The ecosystem demography model (ED), Ecological Monographs, 71(4), 557–585, doi:10.1890/0012-9615(2001)071[0557:AMFSVD]2.0.CO;2, 2001.

Nie, M., Lu, M., Bell, J., Raut, S. and Pendall, E.: Altered root traits due to elevated CO2: a meta-analysis: Root traits at elevated CO2, Global Ecology and Biogeography, 22(10), 1095–1105, doi:10.1111/geb.12062, 2013.

Norby, R. J. and Zak, D. R.: Ecological Lessons from Free-Air CO_2 Enrichment (FACE) Experiments, Annual Review of Ecology, Evolution, and Systematics, 42(1), 181–203, doi:10.1146/annurev-ecolsys-102209-144647, 2011.

Norby, R. J., Sholtis, J. D., Gunderson, C. A. and Jawdy, S. S.: Leaf dynamics of a deciduous forest canopy: no response to elevated CO 2, Oecologia, 136(4), 574–584, doi:10.1007/s00442-003-1296-2, 2003.

O'Brien, E. E., Gersani, M. and Brown, J. S.: Root proliferation and seed yield in response to spatial heterogeneity of below-ground competition, New Phytologist, 168(2), 401–412, doi:10.1111/j.1469-8137.2005.01520.x, 2005.

933 Ordoñez, J. C., van Bodegom, P. M., Witte, J.-P. M., Wright, I. J., Reich, P. B. and Aerts, R.: A
934 global study of relationships between leaf traits, climate and soil measures of nutrient
935 fertility, Global Ecology and Biogeography, 18(2), 137–149, doi:10.1111/j.1466-
936 8238.2008.00441.x, 2009.

937 Oyewole, O. A., Inselsbacher, E., Näsholm, T. and Jämtgård, S.: Incorporating mass flow
938 strongly promotes N flux rates in boreal forest soils, Soil Biology and Biochemistry, 114,
939 263–269, doi:10.1016/j.soilbio.2017.07.021, 2017.

940 Pappas, C., Fatichi, S. and Burlando, P.: Modeling terrestrial carbon and water dynamics across
941 climatic gradients: does plant trait diversity matter?, New Phytologist, 209(1), 137–151,
942 doi:10.1111/nph.13590, 2016.

943 Parton, W., Schimel, D., Cole, C. and Ojima, D.: Analysis of factors controlling soil organic
944 matter levels in Great Plains grasslands, Soil Science Society of America Journal, 51(5),
945 1173–1179, doi:10.2136/sssaj1987.03615995005100050015x, 1987.

946 Phillips, R. P., Brzostek, E. and Midgley, M. G.: The mycorrhizal-associated nutrient economy: a
947 new framework for predicting carbon-nutrient couplings in temperate forests, New
948 Phytologist, 199(1), 41–51, doi:10.1111/nph.12221, 2013.

949 Plomion, C., Leprovost, G. and Stokes, A.: Wood Formation in Trees, PLANT PHYSIOLOGY,
950 127(4), 1513–1523, doi:10.1104/pp.010816, 2001.

951 Poorter, H., Niklas, K. J., Reich, P. B., Oleksyn, J., Poot, P. and Mommer, L.: Biomass allocation
952 to leaves, stems and roots: meta-analyses of interspecific variation and environmental
953 control: Tansley review, New Phytologist, 193(1), 30–50, doi:10.1111/j.1469-
954 8137.2011.03952.x, 2012.

955 Pritchard, S. G., Strand, A. E., McCORMACK, M. L., Davis, M. A., Finzi, A. C., Jackson, R. B.,
956 Matamala, R., Rogers, H. H. and Oren, R.: Fine root dynamics in a loblolly pine forest are
957 influenced by free-air-CO2 -enrichment: a six-year-minirhizotron study, Global Change
958 Biol, 14(3), 588–602, doi:10.1111/j.1365-2486.2007.01523.x, 2008.

959 Raich, J., Rastetter, E. B., Melillo, J. M., Kicklighter, D. W., Steudler, P. A., Peterson, B. J.,
960 Grace, A., Moore, B. and Vorosmary, C. J.: Potential Net Primary Productivity in South
961 America: Application of a Global Model, Ecological Applications, 1(4), 399–429,
962 doi:10.2307/1941899, 1991.

963 Randerson, J., Thompson, M., Conway, T., Fung, I. and Field, C.: The contribution of terrestrial
964 sources and sinks to trends in the seasonal cycle of atmospheric carbon dioxide, Global
965 Biogeochemical Cycles, 11(4), 535–560, doi:10.1029/97GB02268, 1997.

966 Savage, K. E., Parton, W. J., Davidson, E. A., Trumbore, S. E. and Frey, S. D.: Long-term
967 changes in forest carbon under temperature and nitrogen amendments in a temperate
968 northern hardwood forest, Global Change Biology, 19(8), 2389–2400,
969 doi:10.1111/gcb.12224, 2013.

970 Scheiter, S. and Higgins, S. I.: Impacts of climate change on the vegetation of Africa: an
971 adaptive dynamic vegetation modelling approach, Global Change Biology, 15(9), 2224–
972 2246, doi:10.1111/j.1365-2486.2008.01838.x, 2009.

973 Scheiter, S., Langan, L. and Higgins, S. I.: Next-generation dynamic global vegetation models:
974 learning from community ecology, New Phytologist, 198(3), 957–969,
975 doi:10.1111/nph.12210, 2013.

976 Schmidt, G. A., Kelley, M., Nazarenko, L., Ruedy, R., Russell, G. L., Aleinov, I., Bauer, M.,
977 Bauer, S. E., Bhat, M. K., Bleck, R., Canuto, V., Chen, Y.-H., Cheng, Y., Clune, T. L., Del
978 Genio, A., de Fainchtein, R., Faluvegi, G., Hansen, J. E., Healy, R. J., Kiang, N. Y., Koch,
979 D., Lacis, A. A., LeGrande, A. N., Lerner, J., Lo, K. K., Matthews, E. E., Menon, S.,
980 Miller, R. L., Oinas, V., Oloso, A. O., Perlwitz, J. P., Puma, M. J., Putman, W. M., Rind,
981 D., Romanou, A., Sato, M., Shindell, D. T., Sun, S., Syed, R. A., Tausnev, N., Tsigaridis,
982 K., Unger, N., Voulgarakis, A., Yao, M.-S. and Zhang, J.: Configuration and assessment of
983 the GISS ModelE2 contributions to the CMIP5 archive, Journal of Advances in Modeling
984 Earth Systems, 6(1), 141–184, doi:10.1002/2013MS000265, 2014.

985 Shevliakova, E., Pacala, S. W., Malyshev, S., Hurtt, G. C., Milly, P. C. D., Caspersen, J. P.,
986 Sentman, L. T., Fisk, J. P., Wirth, C. and Crevoisier, C.: Carbon cycling under 300 years of
987 land use change: Importance of the secondary vegetation sink, Global Biogeochemical
988 Cycles, 23, GB2022, doi:10.1029/2007GB003176, 2009.

989 Shinozaki, Kichiro, Yoda, Kyoji, Hozumi, Kazuo and Kira, Tatuo: A quantitative analysis of
990 plant form – the pipe model theory. I. Basic analyses, Japanese Journal of Ecology, 14(3),
991 97–105, 1964.

992 Sierra, C. A. and Mueller, M.: A general mathematical framework for representing soil organic
993 matter dynamics, Ecological Monographs, 85(4), 505–524, doi:10.1890/15-0361.1, 2015.

994 Sierra, C. A., Muller, M., Metzler, H., Manzoni, S. and Trumbore, S. E.: The muddle of ages,
995 turnover, transit, and residence times in the carbon cycle, Global Change Biology, 23(5),
996 1763–1773, doi:10.1111/gcb.13556, 2017.

997 Sitch, S., Smith, B., Prentice, I. C., Arneth, A., Bondeau, A., Cramer, W., Kaplan, J. O., Levis,
998 S., Lucht, W., Sykes, M. T., Thonicke, K. and Venevsky, S.: Evaluation of ecosystem
999 dynamics, plant geography and terrestrial carbon cycling in the LPJ dynamic global
1000 vegetation model, Global Change Biology, 9(2), 161–185, doi:10.1046/j.1365-
1001 2486.2003.00569.x, 2003.

1002 Smith, A. R., Lukac, M., Bambrick, M., Miglietta, F. and Godbold, D. L.: Tree species diversity
1003 interacts with elevated CO_2 to induce a greater root system response, Glob Change Biol,
1004 19(1), 217–228, doi:10.1111/gcb.12039, 2013.

1005 Strigul, N., Pristinski, D., Purves, D., Dushoff, J. and Pacala, S.: Scaling from trees to forests:
1006 tractable macroscopic equations for forest dynamics, Ecological Monographs, 78(4), 523–
1007 545, doi:10.1890/08-0082.1, 2008.

1008 Tilman, D.: Plant strategies and the dynamics and structure of plant communities, Princeton
1009 University Press, Princeton, N.J., 1988.

1010 Urbanski, S., Barford, C., Wofsy, S., Kucharik, C., Pyle, E., Budney, J., McKain, K., Fitzjarrald,
1011 D., Czikowsky, M. and Munger, J. W.: Factors controlling CO2 exchange on timescales
1012 from hourly to decadal at Harvard Forest, Journal of Geophysical Research -
1013 Biogeosciences, 112(G2), doi:10.1029/2006JG000293, 2007.

1014 Valentine, H. T. and Mäkelä, A.: Modeling forest stand dynamics from optimal balances of
1015 carbon and nitrogen, New Phytologist, 194(4), 961–971, doi:10.1111/j.1469-
1016 8137.2012.04123.x, 2012.

1017 Vitousek, P. M., Menge, D. N. L., Reed, S. C. and Cleveland, C. C.: Biological nitrogen fixation:
1018 rates, patterns and ecological controls in terrestrial ecosystems, Philosophical Transactions
1019 of the Royal Society B: Biological Sciences, 368(1621), 20130119–20130119,
1020 doi:10.1098/rstb.2013.0119, 2013.

1021 Weng, E., Farrior, C. E., Dybzinski, R. and Pacala, S. W.: Predicting vegetation type through
1022 physiological and environmental interactions with leaf traits: evergreen and deciduous
1023 forests in an earth system modeling framework, Global Change Biology, 23(6), 2482–2498,
1024 doi:10.1111/gcb.13542, 2017.

1025 Weng, E. S., Malyshev, S., Lichstein, J. W., Farrior, C. E., Dybzinski, R., Zhang, T.,
1026 Shevliakova, E. and Pacala, S. W.: Scaling from individual trees to forests in an Earth
1027 system modeling framework using a mathematically tractable model of height-structured
1028 competition, Biogeosciences, 12(9), 2655–2694, doi:10.5194/bg-12-2655-2015, 2015.

1029 Xia, J., Luo, Y., Wang, Y.-P. and Hararuk, O.: Traceable components of terrestrial carbon
1030 storage capacity in biogeochemical models, Global Change Biology, 19(7), 2104–2116,
1031 doi:10.1111/gcb.12172, 2013.

1032 Zea-Cabrera, E., Iwasa, Y., Levin, S. and Rodríguez-Iturbe, I.: Tragedy of the commons in plant
1033 water use, Water Resources Research, 42(6), W06D02, doi:10.1029/2005WR004514,
1034 2006.

1035